Multi-Parametric and Multi-Objective Optimization of Heatsinks for Forced and Natural Convection Based Single-Phase Immersion Cooling of Server

by

TUSHAR ROHIDAS WAGH

Presented to the Faculty of the Graduate School of

The University of Texas at Arlington in Partial Fulfillment of the Requirements

for the Degree of

MASTER OF SCIENCE IN MECHANICAL ENGINEERING

THE UNIVERSITY OF TEXAS AT ARLINGTON

DECEMBER 2021

Supervising Committee:

Dr. Dereje Agonafer

Dr. Miguel Amaya

Dr. Saket Karajgikar

Acknowledgements

December 03, 2021

I would take this opportunity and thank Dr. Dereje Agonafer for his continuous guidance and support through my time in EMNSPC Lab. I am grateful to him for his valuable teachings, opportunities and learnings provided to me in the field of electronic cooling.

I would like to thank Dr. Miguel Amaya and Dr. Saket Karajgikar for being the thesis committee members and providing me with their valuable inputs in improvising my research work.

I would also thank Mr. Satyam Saini, Mr. Pardeep Shahi and Mr. Pratik Bansode for being my tutors and aiding me throughout my research work in EMSPC Lab.

Lastly, I would thank my parents Mr. Rohidas H. Wagh and Mrs. Lalita R. Wagh and my sister Miss. Chanchal R. Wagh for their motivation through my life.

Abstract

Multi-Parametric and Multi-Objective Optimization of Heatsinks for Natural and Forced Convection for Single-Phase Immersion Cooling of Server

(Reprinted with permission © Begell House Inc.)

The University of Texas at Arlington, 2021

Supervising Professor: Dereje Agonafer

An increase in utility of internet-based services, cloud computing and greater performance demands due to rising AI and ML applications have led to a steep growth in GPU and CPU thermal design power. Efficient thermal management of these processors has become a bottleneck in performance enhancement and corresponding power densification of these components. Furthermore, increased pressure on data center owners to reduce power demands and move towards green computing has exacerbated the data center cooling challenges. Single-phase immersion cooling allows data center owners to not only dissipate the increasing heat fluxes efficiently but can also potentially improve equipment reliability as the component are no longer exposed to air, humidity, and airborne contaminants. As a part of thermal design considerations when moving from air to immersion cooling, using optimized heat sinks designed for immersion systems plays a key role in obtaining optimal thermal performance from the CPU or GPU components. An in-depth study of designing such an optimized heat sink is addressed in this investigation. A baseline heat sink solution for an air-cooled Open Compute server was numerically optimized using multi-parametric and multi-objective optimizations. The thermal resistance of the heat sink and pumping power of the system were used as objective functions to obtain a heat sink design by tandem optimization of the fin parameters using optiSLang. The optimizations were carried out under both forced and natural convection flow regimes. Also, a comparison of the difference in optimized geometry of the

heat sink was carried out for aluminum and copper as fin material. The final optimized heat sinks were used to gauge the percentage improvement in thermal performance and reduction in pumping power as compared to the baseline simulations that use an air-cooled heat sink.

List of Illustrations

List of Tables

Table of Contents

Chapter 1 Introduction

In today's digital world, everything revolves around computers, internet and servers. All the functions ranging from internet surfing to data mining takes through the medium of data centers. With the increase in artificial intelligence, machine learning and cryptocurrency there's tremendous need for data processing and data storage. Data has become the world's new currency and efforts are being taken to generate systems that aid in processing and storing data efficiently and swiftly. The function of processing and storing this data is done by high power computational devices called as servers. These servers are equipped with powerful microprocessors that execute billions of operations per second. The server consists of electronic components such as CPU (Central Processing Unit) and GPU (Graphical Processing Unit) which operate at very high TDP (Thermal Design Power). These components generate enormous amount of heat while in operation. The maximum operating temperature for a Silicone chip is 125ºC, the longer exposure to these higher temperatures will have a catastrophic effect on the server. To avoid the failure of servers due to heating issue, the components are required to be cooled so as to maintain the system at optimum operating temperatures. This cooling can be done by a combination of conduction, convection and radiation. Convection stands out to be the most effective mode of heat transfer. A fluid medium is flown/blown over the components in order to cool them. This efficient cooling of servers by having a controlled environment is carried out in a dedicated space known as Data Centers. There are two types of cooling in data centers:

1. Air Cooled Data Centers
2. Liquid Cooled Data Centers

1.1 Air Cooled Data Centers

In the past few decades there has been a tremendous increase in the use of data centers. Almost all of these data centers currently use air as a medium to cool the servers. Lot of research has been done on air cooling ever since. Efforts and studies are being done to increase the efficiency and reduce the effective cost along with its reliability. Generally, air cooled data centers consist of numerous cooling units. For data center applications, servers are piled up in rack, several such racks are organized in a particular manner. There are sub-types in air cooling, raised floor type of air cooling is seen prominently. In raised floor type as the name suggests the floor is raised by a certain height (1 foot approximately) and cold air is made to pass under the raised floor. This cold air in the data center is maintained by Computer Room Air Conditioner (CRAC unit). Due to this the data center gets divided into two sections namely, cold aisle and hot aisle. The cold air is passed from the CRAC unit to the racks from underneath the raised floors. As the cold air gets in close contact with the servers the cold air carries the heat generated by the server thereby cooling the server. But this process converts the cold air into hot air due to the heat transfer and the hot air is then collected by the CRAC unit. The hot air is conditioned by CRAC unit by natural convection and is subsequently cooled down and the cycle gets repeated. External heat exchangers such as chillers are necessary to cool the hot air using fluids. Research studies suggest that almost 30 – 42% of the total energy of a data center is used for cooling operations [1-2]. Since the growth in heat flux in CPUs and GPUs air cooling seems to become obsolete. Also, the average high power usage effectiveness (PUE) for air cooling is 1.58, which denotes inefficient cooling [3]. Due to these factors new cooling methods and technologies such as liquid cooling and other methods are being studied [4-5]. Figure 1 shows arrangement of a typical air-cooled data center

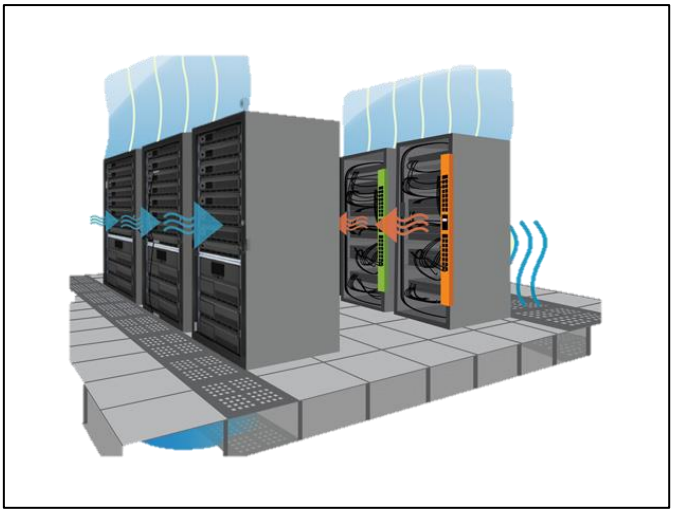

Figure 1 Typical Air-Cooled Data Center

1.2 Liquid Cooled Data Centers

In liquid cooled data centers, a fluid is used to transfer heat generated from the servers to the ambient environment. There are various types of liquid cooled data centers systems are termed as Direct Liquid Cooling (DLC) such as direct-to-chip cooling, Single-Phase Immersion Cooling, Two-Phase Immersion Cooling [6-9]. In today's modern world the importance for greater power multicore CPU and GPU has increased, due to this trend the cooling is moving towards liquid cooling [10-13]. In direct-to-chip type a cold plate is mounted over the heating components CPUs and GPUs and heat exchange takes place by flowing a fluid through the cold plate [14-15]. In Immersion cooled server, heatsinks are mounted over the CPUs and GPUs. The servers are stacked together in a rack and the rack is completely submerged in a dielectric fluid tank called as pods and heat transfers takes place by means of natural convection and if a pump is used to force fluid through the heatsinks it follows forced convection type of cooling of servers. The CDU acts as a pump that supplies fluid to the servers at the required volumetric flow rate and also performs the function of a heat exchanger. The CDU converts the hot fluid carrying the heat from heatsink/cold plate back to cold fluid by the means of external chiller.

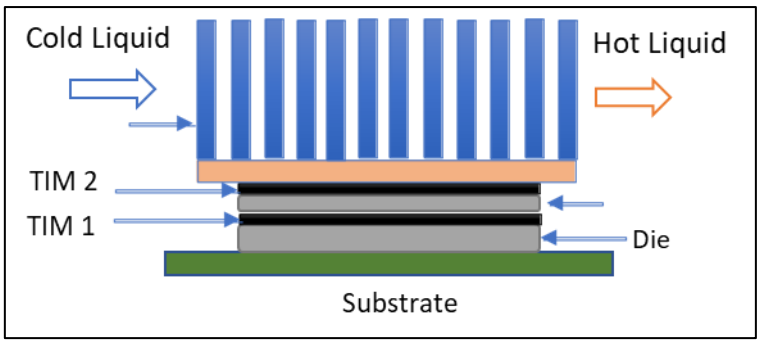

Figure 2 Schematic of Heatsink Placement

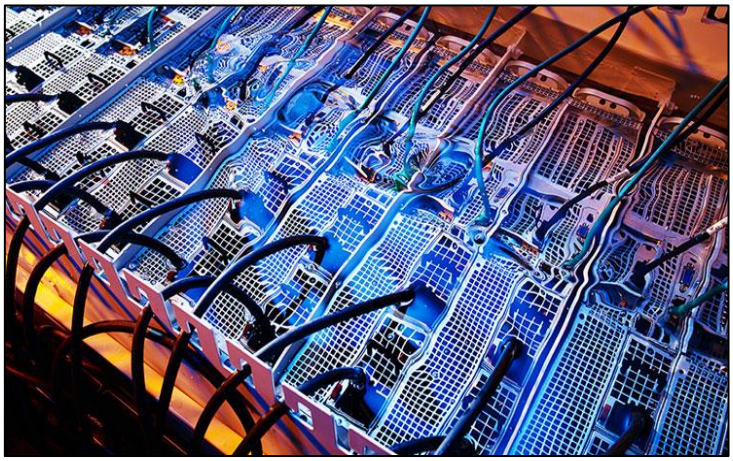

Figure 3 Typical Immersion Cooled Server

1.3 Why Immersion Cooled Data Centers for High Power Data Center?

For many different purposes Immersion Cooling has proved to be an effective solution for high power requirements over the years. Immersion Cooling tends to be a better alternative than air cooling with the technological advancements in CMOS. With Dennard's scaling now vanishing, chip manufacturers are now increasing the number of transistors with the same chip area by compensating on the chip power to generate improved performance. Air is almost 1200 times less effective conductor of heat than fluids, this denotes those fluids can dissipate more amounts of heat than air, thereby increasing the power density. The PUE for single-phase immersion cooling is 1.03. In immersion cooling there are fewer parts than air cooling, due to which there is significant power consumption reduction in immersion cooling and also the reliability of the system increases with decrease in number of moving parts. The major reason immersion cooling has an upper hand over air cooling is that using immersion cooling we can

increase the power density of the data center within the same area as that of an air-cooled data center. Fans in air cooling comply to 20 % of power consumption. Components such as air handling units, humidity controls, fans are eliminated in immersion cooling thereby making it as one of the simplest forms of cooling. The IT components (servers) are sealed off from the external environment size they are submerged in dielectric immersion pods which decreases the reliability failure issues as seen in the contamination of air in air cooled data centers [16-20]. Also, maintaining the humidity of the environment in air-cooled system for optimum performance needs to be taken into consideration [21-22]. Immersion cooling forms much of a plug and play type of system making maintenance and repairing of IT components much easier.

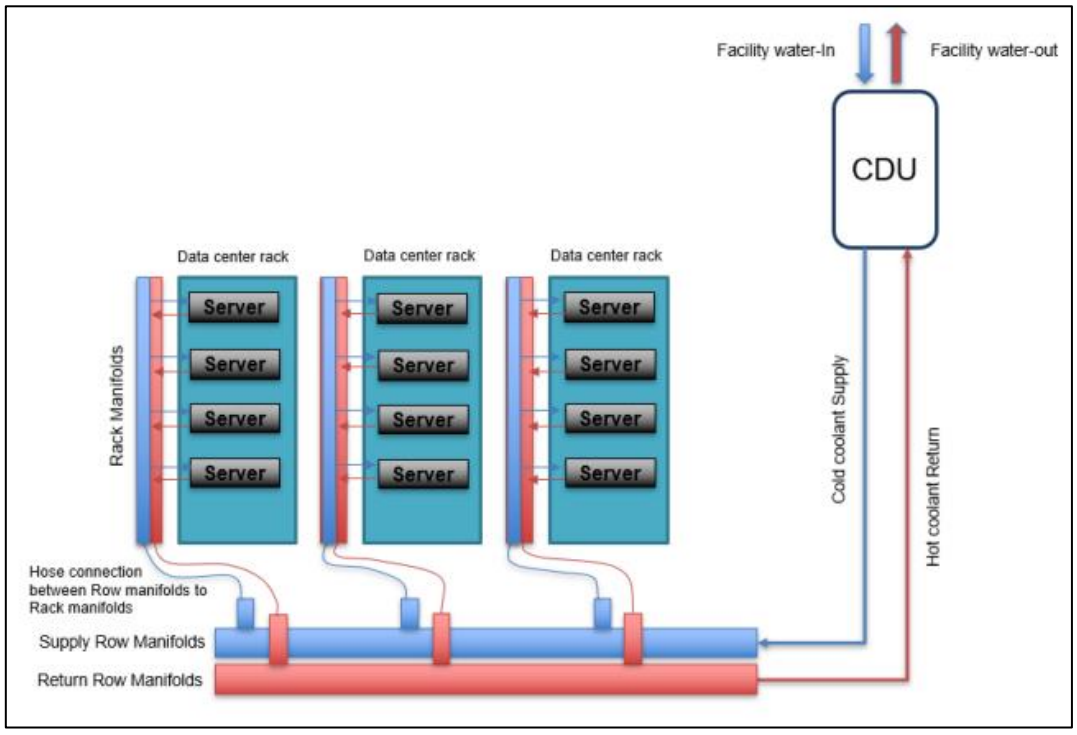

Figure 4 Schematic Diagram of Liquid Cooled Data Center

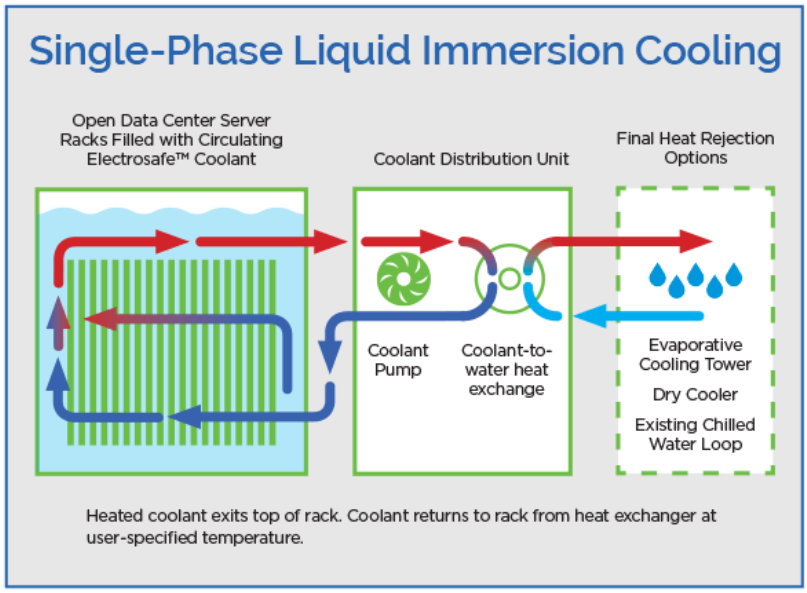

Figure 5 Single Phase Immersion Cooling Layout

Image source: grcooling website

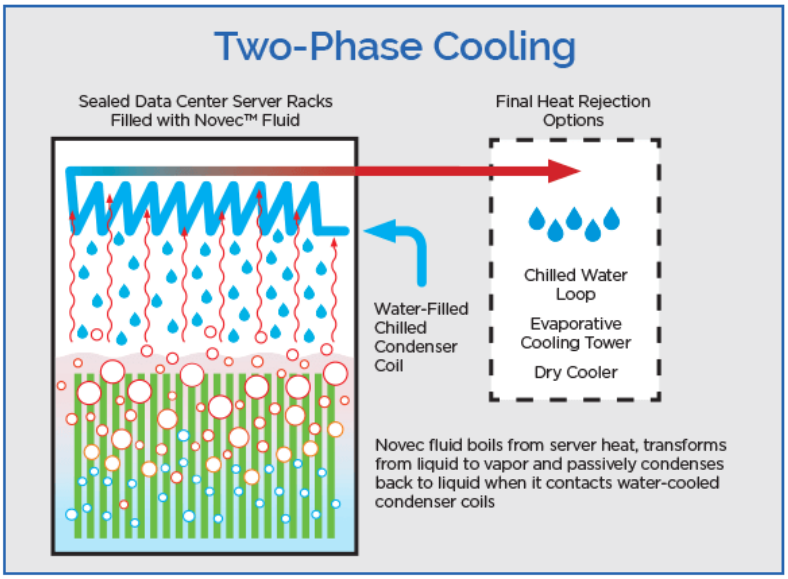

Figure 6 Two Phase Immersion Cooling Layout

Image source: grcooling website

Chapter 2 Objective and Approach of the Study

2.1 Objective of the Study

The primary objective of the study is to optimize parallel plate heatsink used in air cooled server for single-phase immersion cooled server in order to have reduced thermal resistance and pumping power. The optimization of heatsink leads to the improvement in immersion cooling for optimum thermal performance and extremely energy efficient. This study is being performed to understand the effects on server resulting from changing heatsink parameters such as heatsink height, heatsink fin thickness, number of fins thereby varying the surface area and impedance to the fluid flow through the heatsink of the server. In order to generate optimized heatsink with reduced pumping power of fluid across the heatsink the pressure drop is taken into consideration by keeping the flow rate constant. To compare the optimized heatsink with the existing heatsink in immersion cooling setup. Understanding the overall effect on the server by changing the heatsink material from Aluminum to Copper, comparing the advantage and disadvantages between the two materials. To analyze the effectiveness of Electro Cool-100 (EC-100) a synthetic dielectric fluid used as the fluid for single-phase immersion cooling of servers. Understanding the concept of thermal shadowing, ill effects of thermal shadowing of the overall system. To optimize heatsink so as to reduce thermal shadowing and cooling the second heatsink in an efficient manner.

2.2 Approach of the Study

Firstly, the server was modelled using ANSYS Icepak 2020 R2 version. After modelling, grid independence study was performed on modelled server and the mesh parameters were confirmed. Next with the mesh parameters chosen from grid independence study the model was validated with the baseline model. Boundary conditions for optimization were set as per forced and natural condition cases. Then preliminary run with Aluminum heatsink was performed. Post processing of the results was done and were published in ANSYS optiSLang

version 7.3. Optimization solver and design parameters were set in ANSYS optiSLang. After solving all the design points the results were analyzed, optimum results were found, comparison were made and conclusion for this study was found.

Chapter 3 Model Validation, Grid Independence Study and Calculations

3.1 Server Description

For this study “Third Generation Open Compute Winterfell Server” is considered. The server consists of 4 Dual In-line Memory Module (DIMM) of 8 GB memory. It has two microprocessors with TDP of 115 W each. The server has two CPUs each of 50 mm x 50mm dimensions. The chassis dimensions are 511 mm x 167 mm x 96 mm (length x width x height). This Open Compute Server has a form factor of 2 rack unit [23].

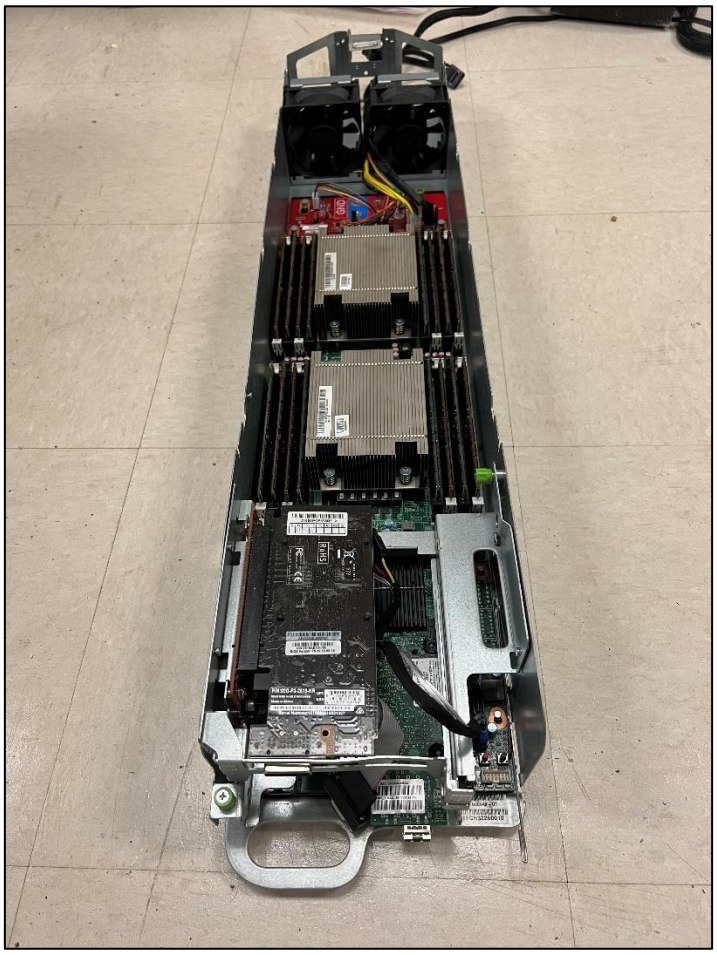

Figure 7 Winterfell Server

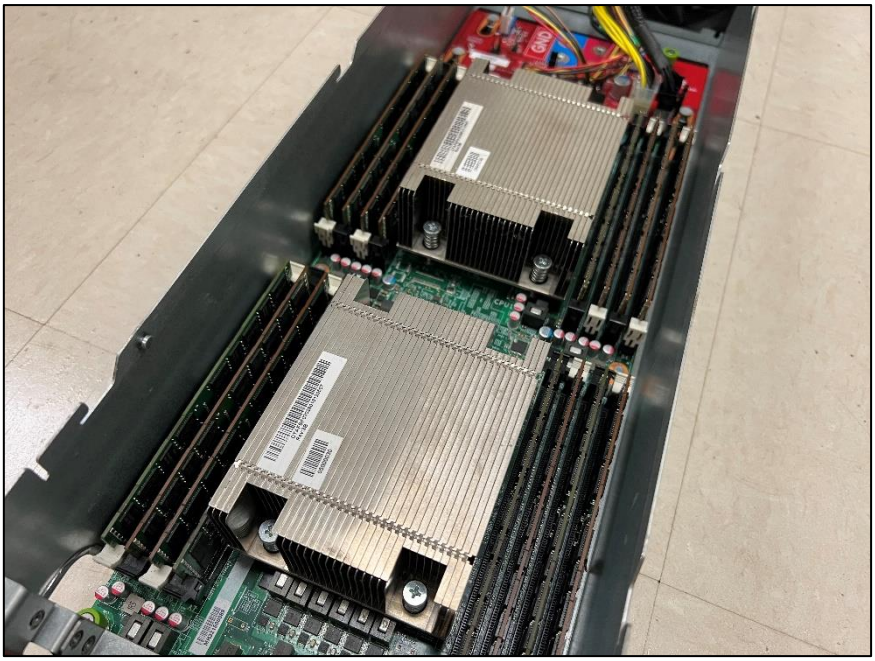

Figure 8 Heatsink in Winterfell Server

Table 1 Server Rack Unit Dimensions

Server	Rack Unit (mm)	Open Rack Unit (mm)	Heatsink Overall Height (mm)
1U	44.5	48	41
1.5U	66.5	72	35
2U	89	96	26

3.2 Baseline Server Model Description

ANSYS Icepak 2020 R2 version was used to perform the Computational Analysis [24]. Since, ANSYS is the best tool for analysis of the model thereby helping in knowing the Engineering Characteristics. Few changes were made to the actual server for the study. The baffle to direct the air flow through the heatsink is excluded since it is not necessary for immersion cooling. Since we are varying the heatsink parameters (i.e., heatsink height, heatsink fin thickness,

heatsink number of fins) the height of the cabinet depends upon the overall height of the heatsink. Two fans for air cooling are omitted.

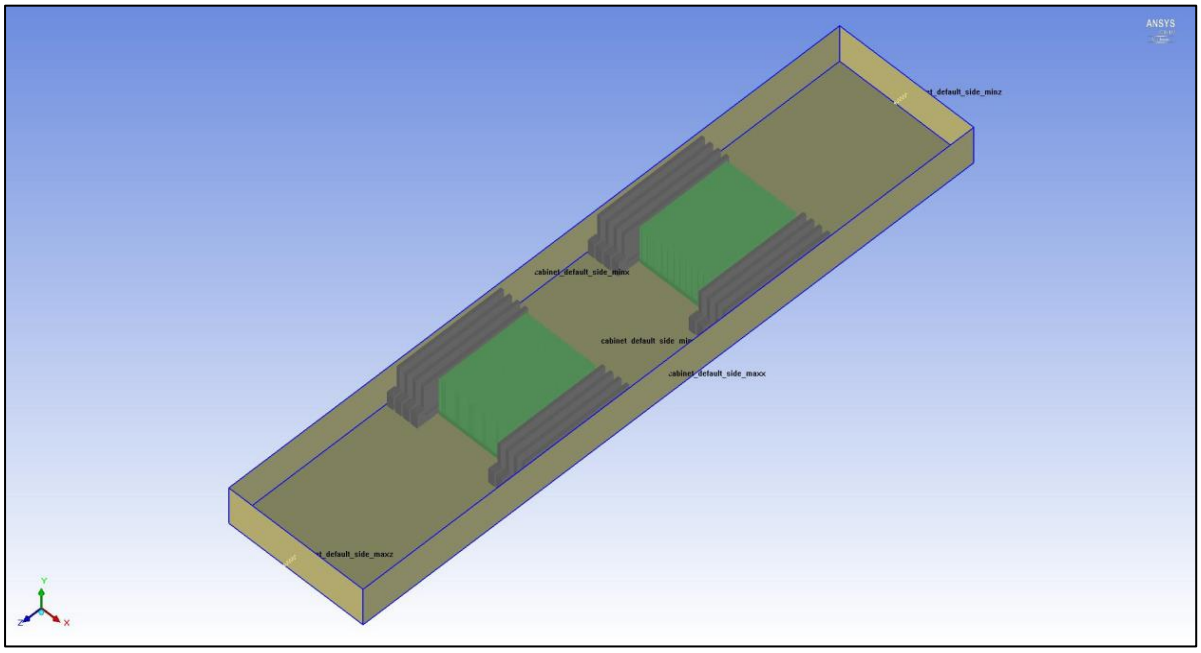

Figure 9 Isometric View of Baseline Model

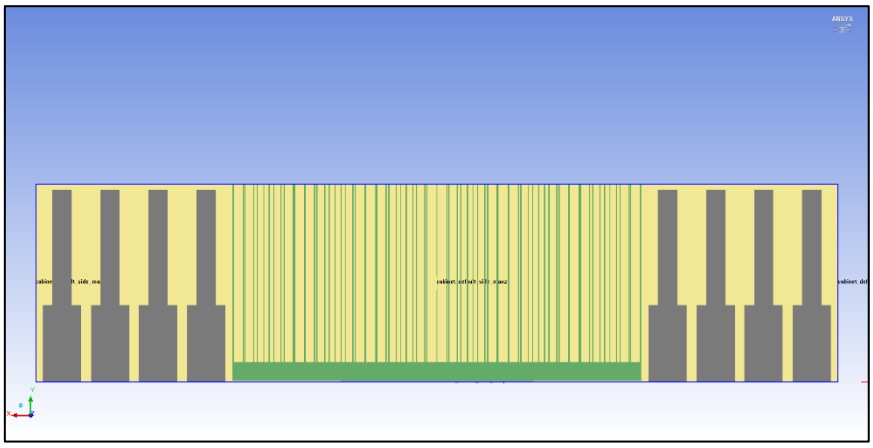

Figure 10 Front View of Baseline Model

The chassis dimensions are 1000 mm x 167 mm x 41.2 mm (length x width x height). Since this study is more focused towards the optimization of heatsink the overall length of the server does not influence the results.

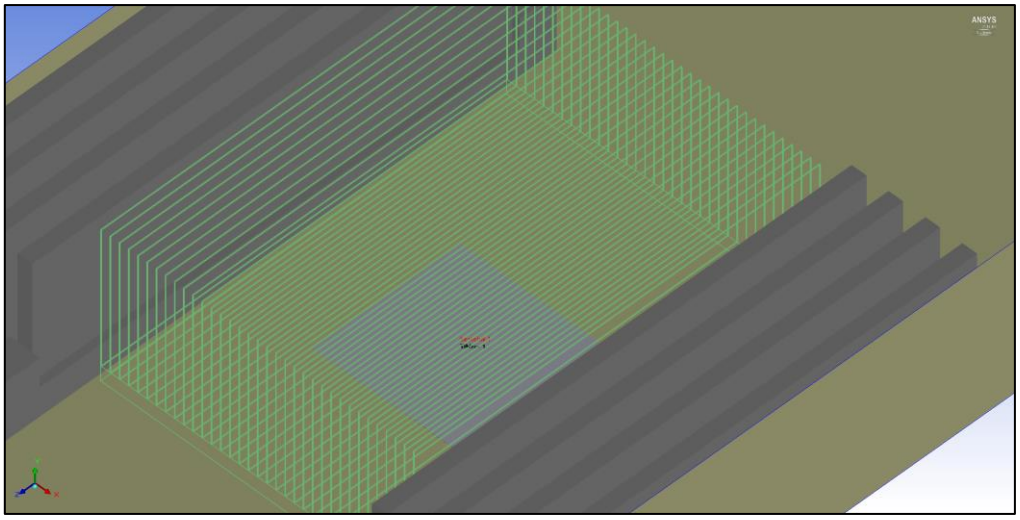

Figure 11 Heatsink

To thoroughly optimize the heatsink for pumping power the cabinet height is 0.2 mm above the overall heatsink height. The inlet of the server is in the negative Z direction and the outlet is in the positive Z direction.

Table 2 Baseline Model Components and Properties

Component	Dimension
Server (L x W x H)	1000 mm x 167 mm x 41.2 mm
Number of CPUs	2
CPUs	50 mm x 50 mm
TDP for each CPU	115 W
Heatsink type	Parallel Plate Type Heatsink
Heatsink Base	110 mm x 85 mm
Heatsink Base Thickness	4 mm
Heatsink Fin Height	37 mm
Heatsink Fin Thickness	0.23 mm
Number of Fins	35
Heatsink Overall Height	41 mm
TIM Conductivity	3.8 W/m-K
TIM Specific Heat	1000 J/kg-K

3.3 Calculations

3.3.1 Area of Baseline Model

$$\text{Area} = \text{Width} \times \text{Height}$$

$$= 167 \text{ (mm)} \times 41.2 \text{ (mm)}$$

$$= 6880.4 \text{ mm}^2$$

$$= 6880.4 \times 10^{-6} \text{ m}^2$$

3.3.2 Perimeter of Baseline Model

$$\text{Perimeter} = 2 \times (\text{Width} + \text{Height})$$

$$= 2 \times (167 \text{ mm} + 41.2 \text{ mm})$$

$$= 416.4 \text{ mm}$$

$$= 0.4164 \text{ m}$$

3.3.3 Hydraulic Diameter of Baseline Model

$$\text{Hydraulic Diameter} = 4 \times \text{Flow Area} / \text{Wetted Perimeter}$$

$$= 4 \times 6880.4 \times 10^{-6} \text{ (m}^2\text{)} / 0.4164 \text{ (m)}$$

$$= 0.06609 \text{ m}$$

3.3.4 Volumetric Flow Rate

For our study we consider Volumetric Flow Rate of 2 Liters Per Minute (LPM)

$$1 \text{ LPM} = 1.6667 \times 10^{-5} \text{ m}^3/\text{sec}$$

$$1.5 \text{ LPM} = 2.5 \times 10^{-5} \text{ m}^3/\text{sec}$$

$$2 \text{ LPM} = 3.333 \times 10^{-5} \text{ m}^3/\text{sec}$$

3.3.5 Velocity Calculation

We consider Volumetric Flow Rate of 2 LPM, velocity of the fluid can be calculated as follows

$$\text{Volumetric Flow Rate} = \text{Area} \times \text{Velocity}$$

$$\text{Velocity} = \text{Volumetric Flow Rate} / \text{Area}$$

$$= 3.333 \times 10^{-5} \ (m^3/sec) / 6880.4 \times 10^{-6} \ (m^2)$$

$$= 0.004844 \ m/sec$$

3.4 Synthetic Fluid EC – 100

For this study we used Electro Cool 100 a dielectric synthetic fluid from Engineered Fluids. The major reason to use EC – 100 was that model validation could be done since the experimental test on server was performed using EC – 100 [25]. Also, the fluid is suitable for general electronics cooling, has excellent material compatibility, high dielectric strength, good heat transfer and is biodegradable.

Table 3 EC-100 Fluid Properties

Temperature	Kinematic Viscosity (ν)	Dynamic Viscosity (η)	Density (ρ)	Thermal Conductivity (K_f)	Specific Heat
°C	$m^2/sec \ (10^{-6})$	kg/m – sec	kg/m^3	W/m – K	J/kg – K
0	74.26	0.06382	859.06	0.1404	2.0577
10	42.04	0.03583	852.46	0.13965	
20	25.93	0.02193	845.86	0.1389	
30	17.14	0.01439	839.26	0.13815	
40	11.99	0.00998	832.66	0.13665	2.209
50	8.78	0.00725	826.06	0.13559	
60	6.68	0.00547	819.46	0.13515	

3.5 Grid Independence Study

For the model to be accurate grid independence study is performed for single-phase immersion cooled server. For this study the TDP of 115 W was set for each CPU, the inlet temperature of the fluid was set at 30° and the inlet velocity was kept at 0.004844 m/sec.

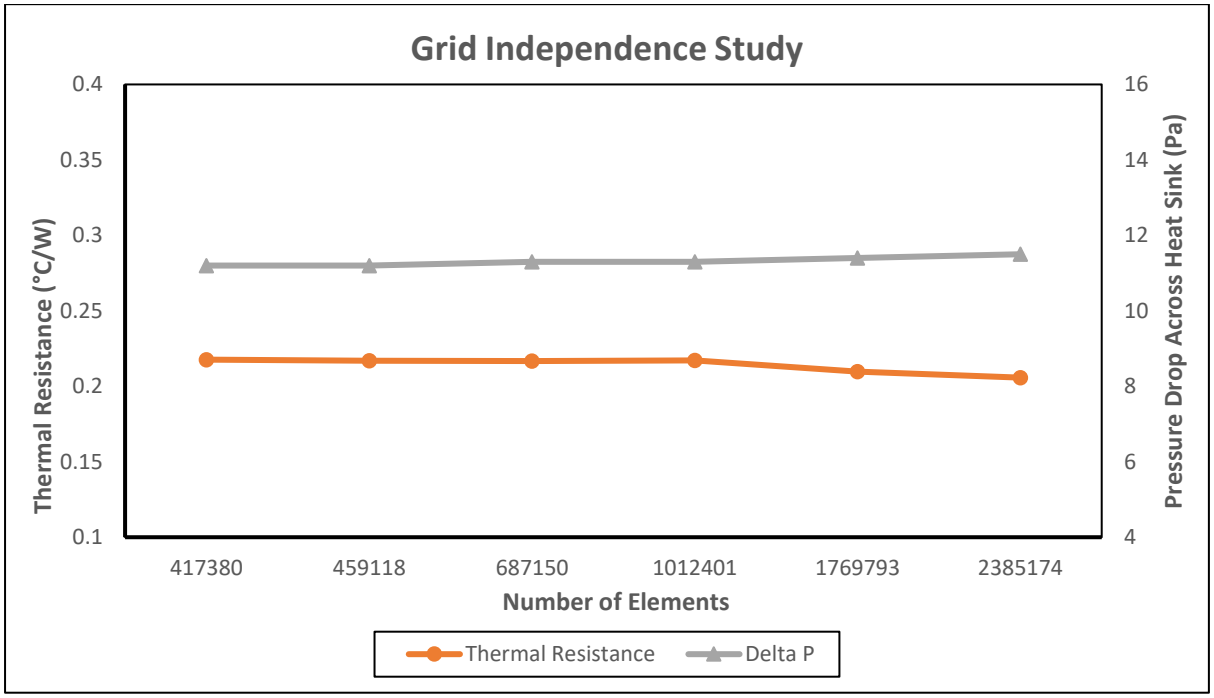

Figure 12 Grid Independence Study

ANSYS Icepak performs meshing at 1:20 ratio at default. The mesh analysis was done at 1:5, 1:10, 1:20, 1:30, 1:50, 1:60 ratios and the time taken by the respective ratios was 13, 19, 28, 44, 62, 79 minutes. The thermal resistance for the model remains almost equal with slight decrease in the latter ratios. The percentage decrease in thermal resistance is not that significant. The pressure drop across the heatsink seems to be stable until the 1:30 ratio whereas, it slightly increases at the 1:50 and 1:60 ratio, but the percentage increase in insignificant. Hence, the ratio of 1:30 at 1012401 number of elements was selected.

3.6 Computational Model Validation

3.6.1 Model Validation

Experimental study of third generation open compute servers for single-phase immersion cooling was performed by previous master's student Trevor McWilliams [26]. The computational model sever was validated by performing simulation for fluid inlet temperatures of 30ºC and 40ºC at 115 W of TDP (100% use) at various flow rates and comparing their average junction temperatures.

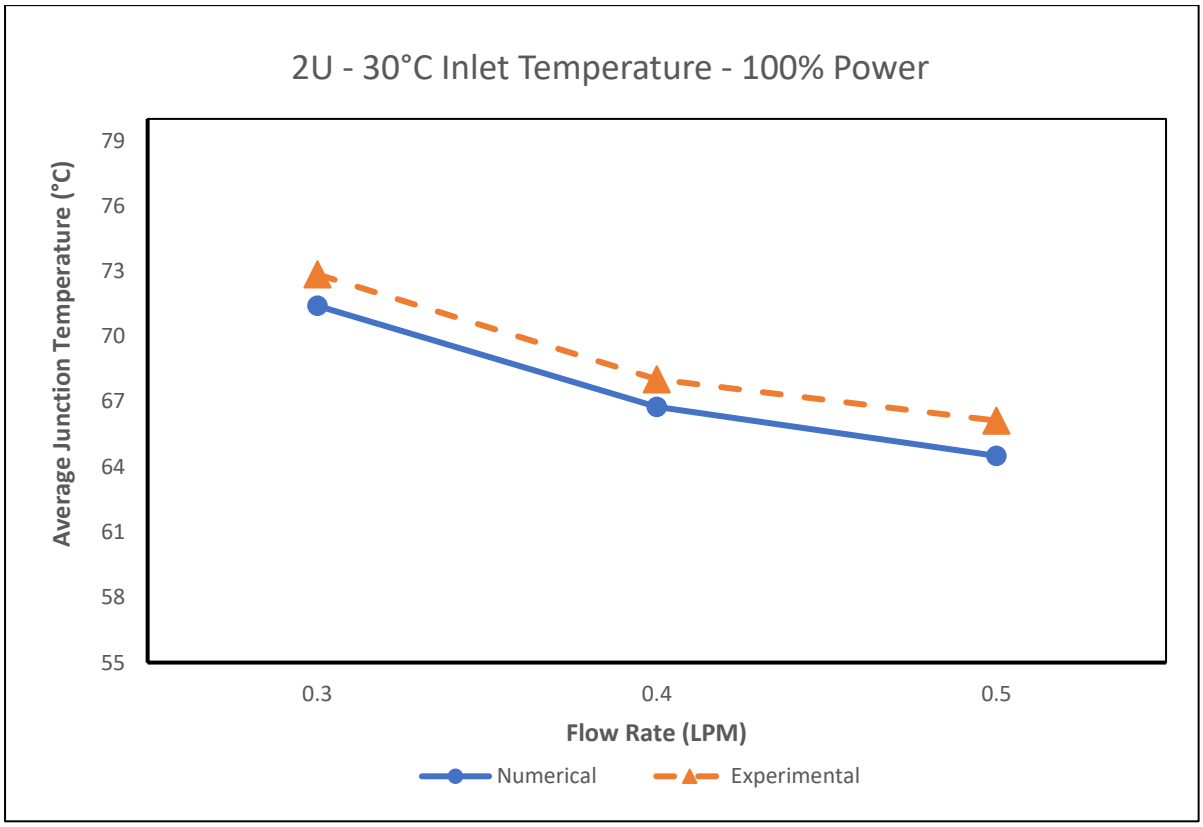

Figure 13 Model Validation @ 30ºC Inlet Temperature

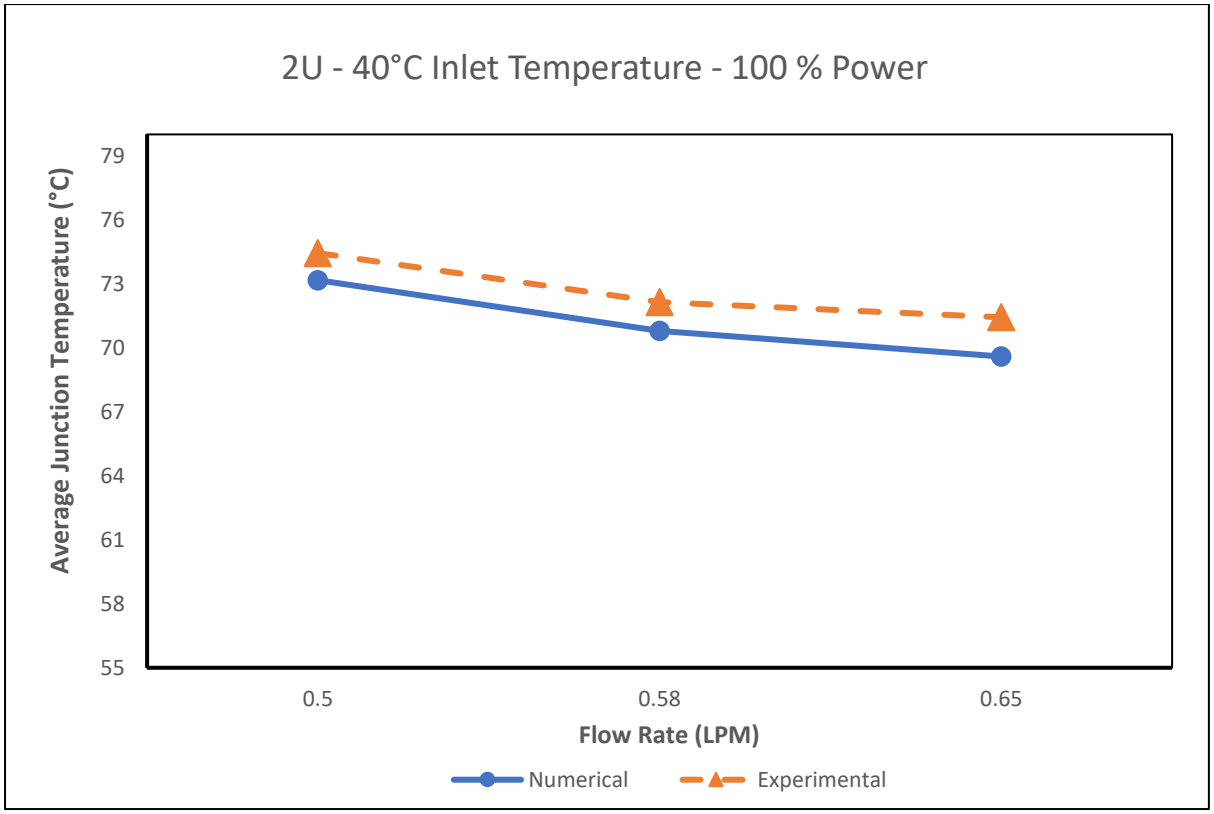

Figure 14 Model Validation @ 40ºC Inlet Temperature

The results of the computational (numerical) model aligned well with the experimental results. The reason for slight difference could be due to loss of heat due to the surroundings (boundary conditions) while conducting the experiment.

3.6.2 Reynolds Number (Re)

Reynolds number is a dimensionless number that describes the type of flow associated with the geometry. Reynolds number can be calculated by using the formula

$$\text{Reynolds Number} = (\text{Velocity} \times \text{Hydraulic Diameter}) / \text{Kinematic Viscosity}$$

$$Re = V \times D / \nu$$

$$= (0.004844 \times 0.06609) / (17.14 \times 10^{-6})$$

$$= 18.6779$$

Since Re = 18.6779; 0 < Re < 2000 the flow is Laminar type.

3.6.3 Prandtl Number

Prandtl number is a dimensionless number that is dependent upon the fluid and fluid state. It describes if thermal diffusivity dominates (if Pr << 1) or momentum diffusivity dominate (if Pr >> 1) the behavior. Prandtl number is calculated as follows

$$\text{Prandtl Number} = \text{Momentum Diffusivity} / \text{Thermal Diffusivity}$$

$$\text{Prandtl Number} = (C_p \times \mu) / K$$

$$= (0.01439 \times 2.101)/0.13815$$

$$= 0.2188$$

Since Prandtl number is << 1 thermal diffusivity dominates the behavior.

3.6.4 Thermal Shadowing

Thermal shadowing is a concept in which the heat carrying capacity of the medium decreases from one heat source to the next. Thermal shadowing in this study is be explained with the picture. Cold fluid enters heatsink – 1 extracts a certain amount of heat thereby increasing its own temperature in the process, which makes the cold fluid turn into hot fluid. Some of the cold liquid bypasses the heatsink – 1 and enters the region between heatsink 1 and 2 [27-28].

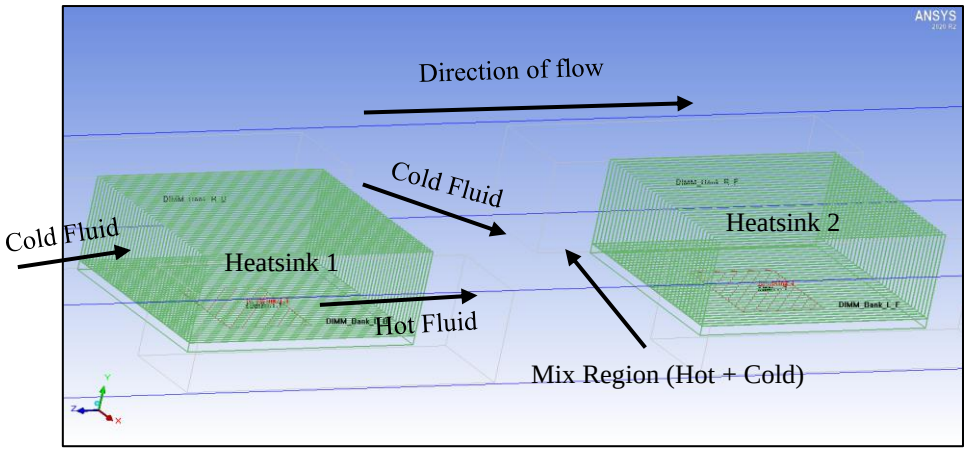

Figure 15 Thermal Shadowing

The hot and cold fluid mixes in the region between heatsink 1 and 2 and is called as the mix region. Due to this there is a temperature difference between the temperature of cold fluid before entering heatsink – 1 and the mixed fluid (hot + cold). The cold fluid already carrying heat from heatsink – 1 cannot extract the same amount of heat from heatsink – 2 due to rise in its own temperature. Due to thermal shadowing the temperature of heatsink – 1 will always be less than the temperature of heatsink – 2 [29].

3.6.5 Thermal Resistance

Thermal Resistance is one of the most important aspects in designing a cooling system. Thermal Resistance is calculated as;

Thermal Resistance = (Junction Temperature – Inlet Fluid Temperature) / Heat Dissipation

Thermal Resistance = $(T_j - T_a)$ (°C) / Power (W)

3.6.6 Pressure Drop

Pressure Drop across the heatsink is the measure of loss of pressure of a fluid by its journey through a heatsink. Pressure drop is an important factor in deciding the pumping power. The pumping power is a product of volumetric flow rate of the fluid times the pressure drop across the system. In our study for forced convection case the volumetric flow rate of the fluid is set constant at 2 LPM, thereby pumping power becomes a function of pressure drop across the heatsink.

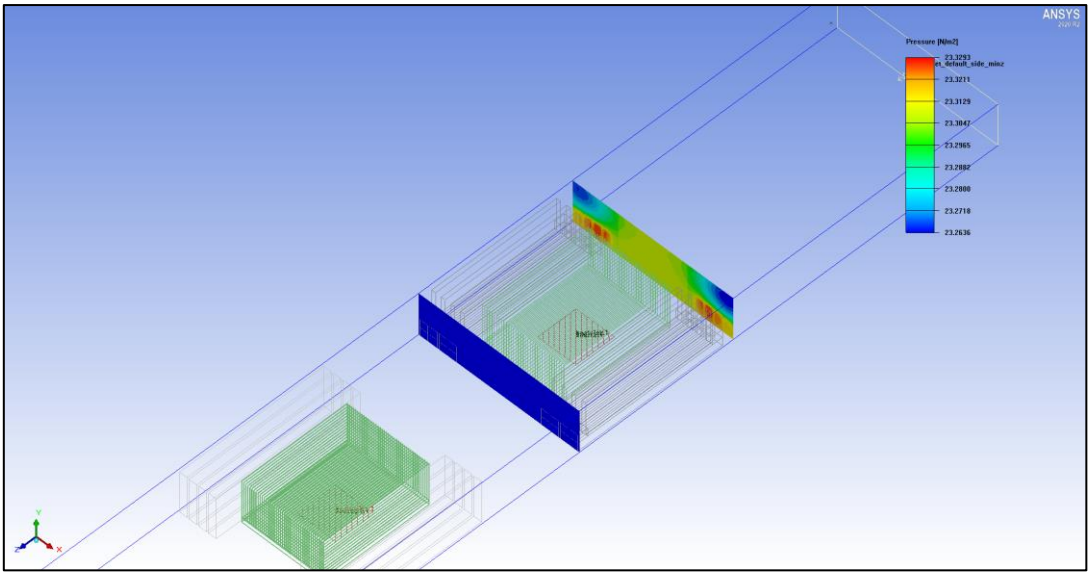

Figure 16 Pressure Drop Across Heatsink

The pressure drop is measured by placing cut plane of pressure 25 mm before and after the heatsink in post processing. The pressure drop is calculated by taking the difference between the mean values of cut plane before and after the heatsink.

3.7 Parameters for Optimization

3.7.1 Input Parameters for Optimization

For the optimization of the heatsink for single-phase immersion cooling various physical parameters of the server, heatsink and other components must be taken into consideration. There are constant input parameters, variable input parameters required for optimization and the resulting output parameters.

Table 4 Constant Input Parameters

Number	Constant Input Parameter	Value
1	TDP for each CPU	115 W
2	Fluid Flow Rate	2 LPM
3	Fluid Inlet Temperature	30ºC
4	Heatsink Base Area	85 mm x 110 mm
5	Heatsink Base Height	4 mm

To understand the effects of form factor reduction of heatsink on the overall sever, the server cabinet height must be maintained accordingly. The server cabinet height is set at +0.2 mm than the overall heatsink height for this study.

Table 5 Variable Input Parameters

Number	Variable Input Parameter	Reason for Variation
1	Fluid Inlet Velocity	Change in Cabinet Height Dimension
2	Overall Heatsink Height	For Heatsink Optimization
3	Heatsink Fin Thickness	For Heatsink Optimization
4	Heatsink Number of Fins	For Heatsink Optimization

Depending upon the constant and variable input parameters the resulting output parameters are generated. The output parameters that are important for this study are taken into consideration.

3.7.2 Variable Heatsink Input Parameters

As mentioned in table few input parameters of the heatsink geometry are varied so as to generate best possible combination of parameters to design optimum heatsink with least thermal resistance and pressure drop.

Table 6 Design Points

Number	Overall Heatsink Height (mm)	Heatsink Fin Thickness (mm)	Heatsink Number of Fins
1	26	0.23	25
2	29	0.32	27
3	32	0.41	29
4	35	0.5	31
5	38	0.59	33
6	41	0.68	35
Step Size	3 mm	0.09 mm	2 fins
Total Discrete Values	6	6	6
Total Number of Design Points = 6 x 6 x 6 = 216			

The total number of design points generated are 216. This depicts those 216 combinations are possible upon varying the heatsink geometry parameters. Study is being performed to find the best possible solution from these 216 design points for different cases.

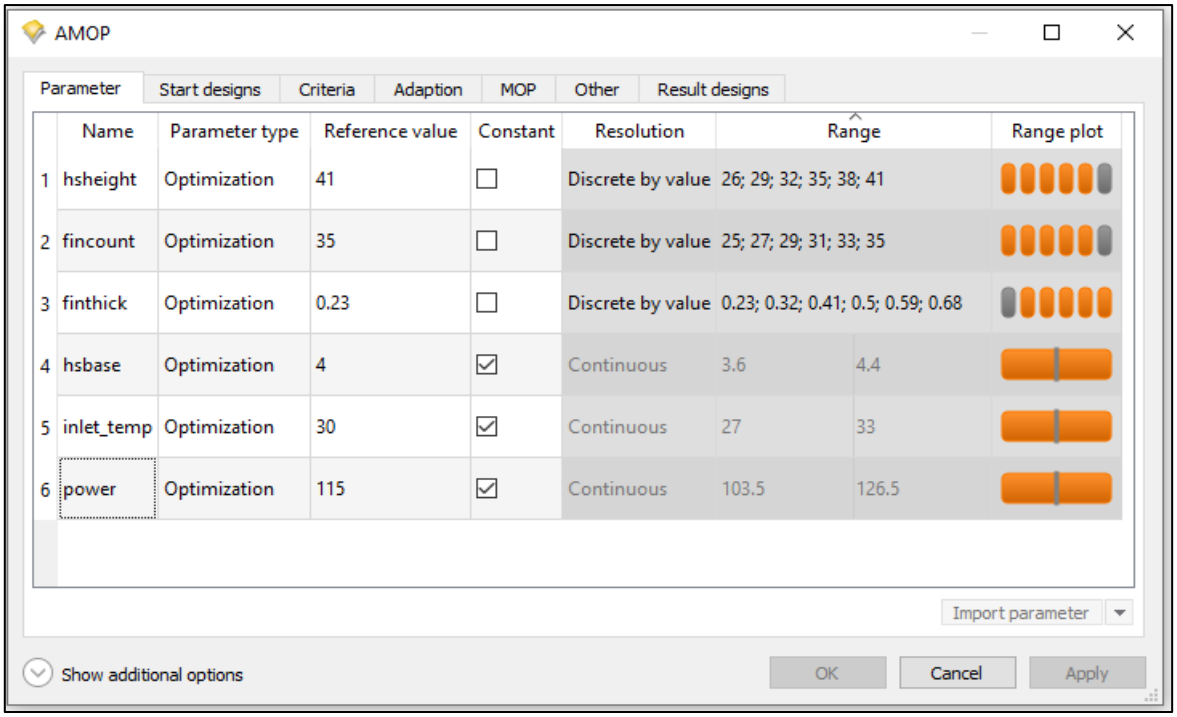

Figure 17 Design Points in optiSLang

3.8 Boundary Conditions for Forced Convection

The server is analyzed for forced convection type of cooling. Inlet is set in the negative Z direction and the outlet is set in positive Z direction. With the walls set as adiabatic wall. The fluid inlet temperature is 30ºC with a volumetric flow rate of 2 LPM, the velocity corresponds to 0.004844 m/sec. The TDP of each CPU is set at 115 W. Gravity is acting in the negative Y direction (downward). Static Pressure is set to 1 atmospheric.

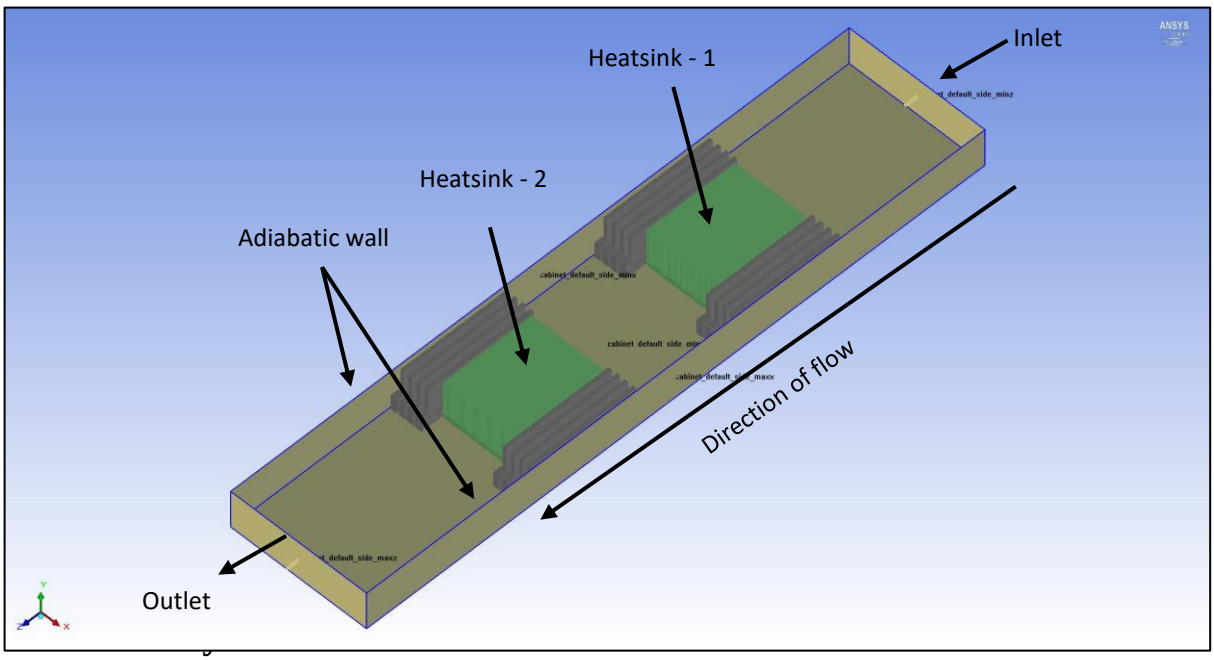

Figure 18 Boundary Condition for Forced Convection

3.9 Boundary Conditions for Natural Convection

The server along with forced convection is analyzed for natural convection and the heatsink is optimized for both the type of convection. The boundary condition for natural convection is as follows; the inlet and outlet of the server are set as openings. There is no volumetric flow rate set since this is a case of natural convection. The flow is gravity/buoyancy based. The fluid temperature is set at 30ºC. The static pressure is set at 1 atmosphere. The TDP for each CPU is set at 115 W. Gravity is acting in the negative Z direction.

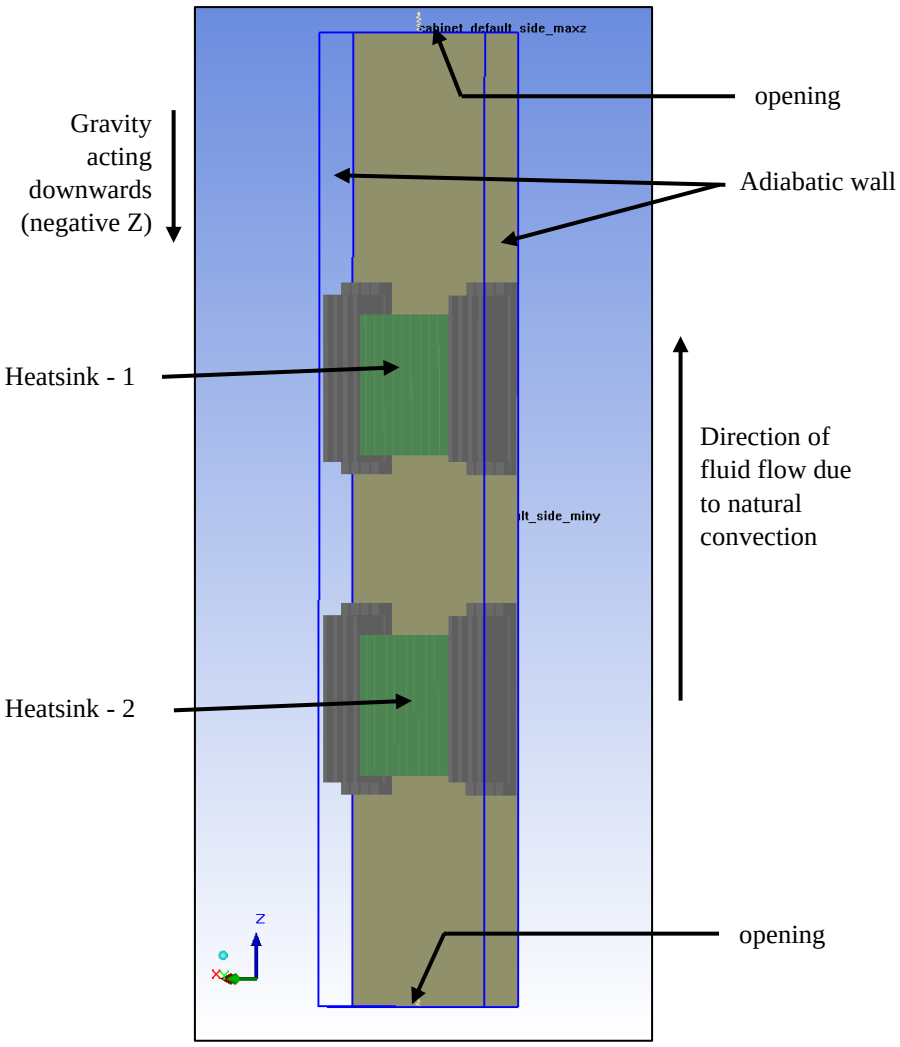

Figure 19 Boundary Condition for Natural Convection

3.10 Optimization using optiSLang

optiSLang is a Computer Aided Engineering (CAE) software platform wherein sensitivity analysis, multi-disciplinary optimization and robustness analysis can be performed. In this study optiSLang is used for the optimization of heatsink of server for forced and natural convection cases for single-phase immersion cooling. The solver uses Adaptive Metamodel of Optimum Prognosis (AMOP) [30]. In AMOP the prediction quality of the surrogate model is increased if unimportant input parameters are removed. The surrogate model finds the optimum input value so as to match the required optimization set by the user, using appropriate

approximation (moving least squares with linear or quadratic regression basis) model. The criteria for optimization in our study is set as two objectives namely, a) MINIMIZE thermal resistance and b) MINIMIZE pressure drop across heatsink.

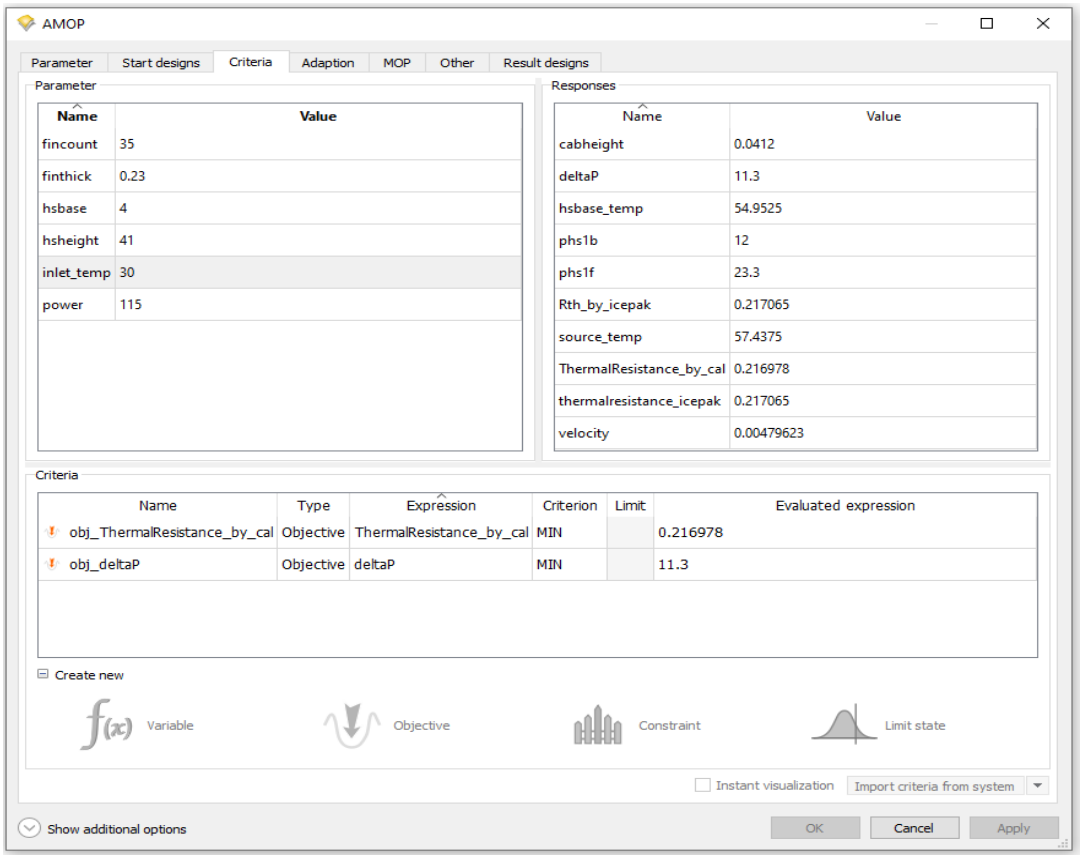

Figure 20 Criteria For Optimization in optiSLang

Chapter 4 Results and Discussion

4.1 Results of Baseline Model for Forced Convection using Aluminum Heatsink

Table 7 Model Parameters for Forced Convection

Parameter	Value
Fluid Inlet Temperature	30ºC
TDP for each CPU	115 W
Volume Flow Rate of Fluid	2 LPM
Velocity of Fluid at Inlet	0.004844 m/sec
Static Pressure	1 atmosphere
Heatsink Base Area	85 mm x 110 mm
Heatsink Base Height	4 mm
Heatsink Fin Height	37 mm
Heatsink Fin Thickness	0.23 mm
Heatsink Number of Fins	35
Thermal Resistance	0.21698 ºC/W
Pressure Drop	11.3 Pa
Heatsink Base Temperature	54.9527 ºC
Source Temperature	57.437 ºC

4.2 Results for Forced Convection Case using Aluminum Heatsink

As mentioned, 216 design points were generated in optiSLang. These 216-design point were simulated in ANSYS Icepak. The fluid inlet temperature, TDP for each CPU, Volume Flow Rate of Fluid, Heatsink Base Area, Heatsink Base Height were kept constant whereas heatsink fin thickness, heatsink fin height and number of fins were varied as mentioned in table. The boundary conditions for forced convection case is explained in section 3.8.

4.2.1 Total Effects for Forced Convection for Aluminum Heatsink

optiSLang describes the percentage effects of variable input parameters upon the output of the system.

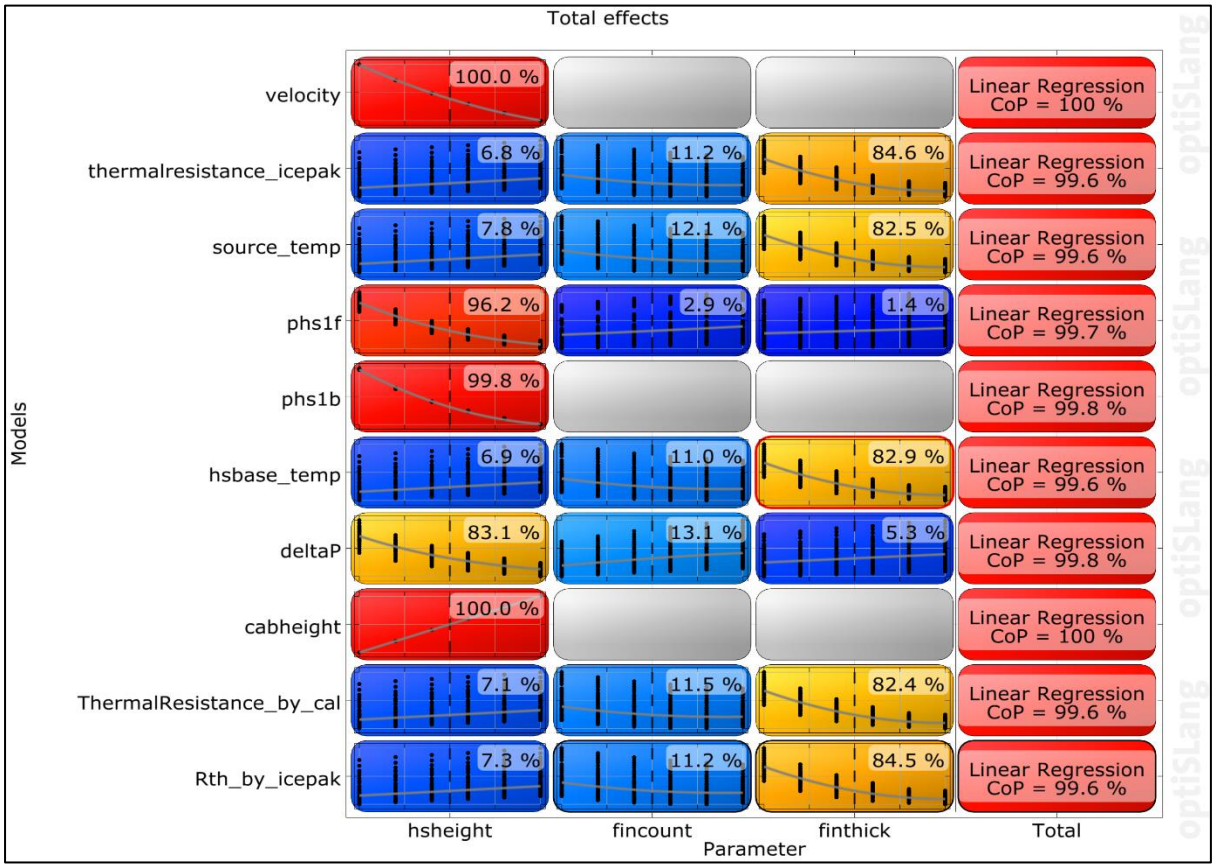

Figure 21 Total Effect for Forced Convection for Aluminum Heatsink

The above figure describes that the output/objective parameter thermal resistance (ThermalResistance_by_cal) is influenced 82.4 % by heatsink fin thickness, 11.5 % by heatsink

number of fins and least influenced by 7.1% by heatsink height. Whereas as the other objective parameter pressure drop (deltaP)is influenced majorly by heatsink height 83.1 %, moderately by heatsink number of fins 11.0 % and least by heatsink fin thickness 5.3 % With this it is evident that the major influencing input parameter for thermal resistance is the least influencing input parameter for pressure drop and vice-versa. Through this we can decide that thermal resistance and pressure drop are inversely proportional to each other i.e., if you tend to improve thermal resistance, the pressure drop will worse and vice-versa.

4.2.2 Response graphs for Forced Convection

The response graphs of the thermal resistance and pressure drop against the three varying input parameters is mentioned. The thermal resistance decreases with increase in heatsink fin thickness whereas it increases with increase in heatsink fin height

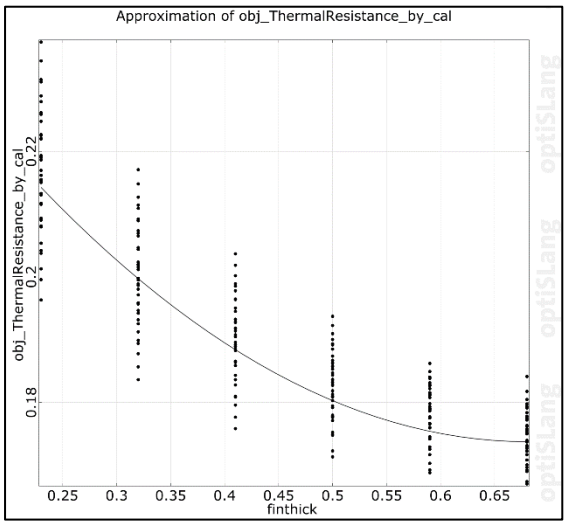

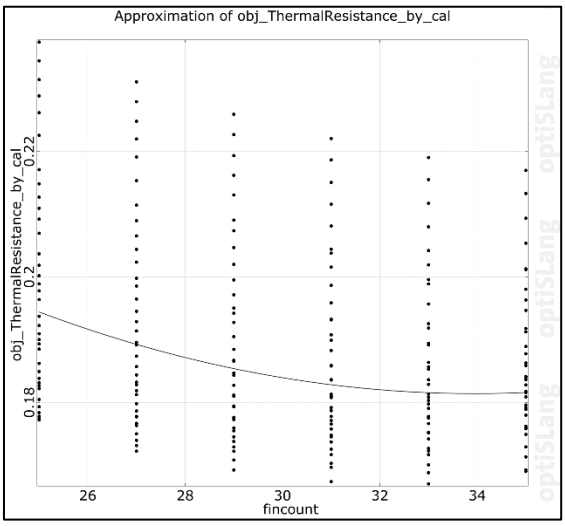

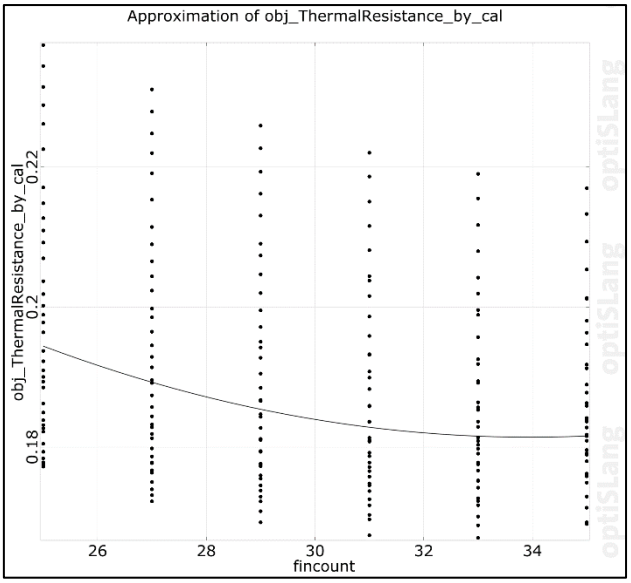

Figure 22 Response Curves for Thermal Resistance for Forced Convection

The pressure drop across the heatsink in forced convection decreases with increase in heatsink fin height and it increase with increase in heatsink number of fins and increase gradually with heatsink fin thickness

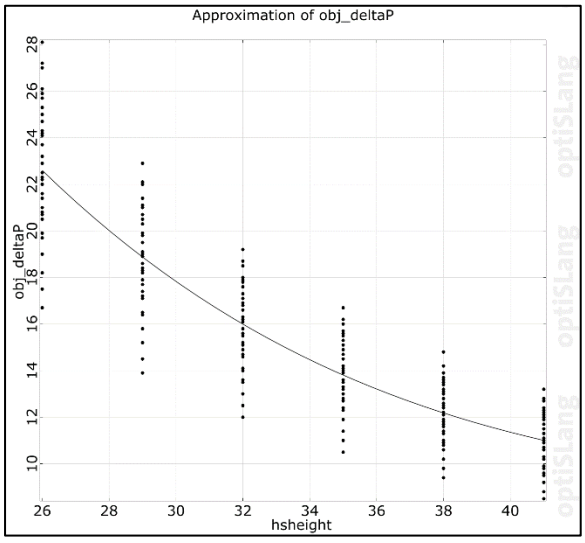

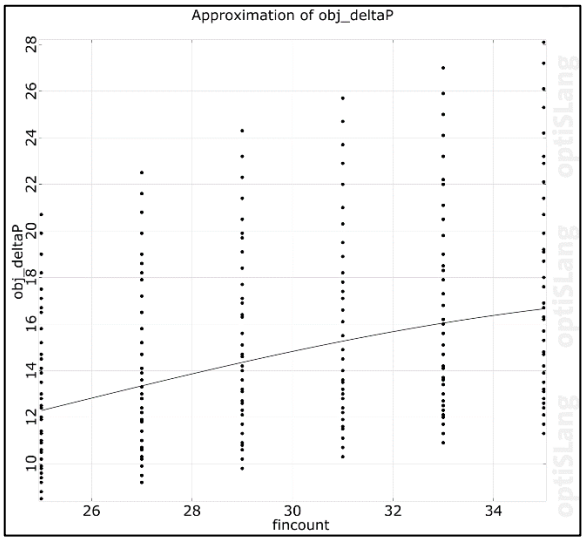

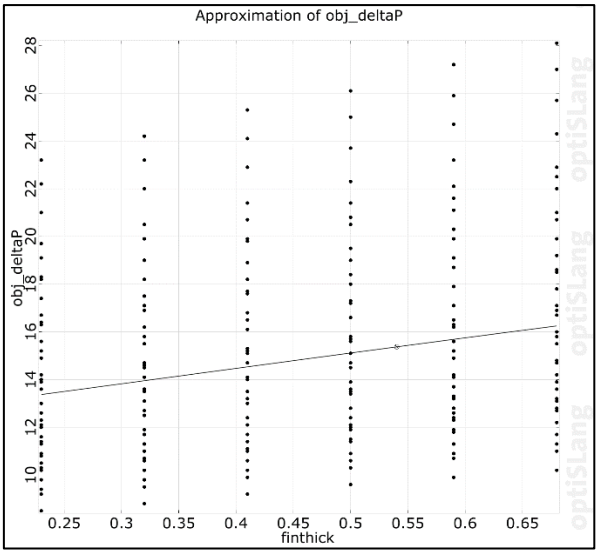

Figure 23 Response Curves for Pressure Drop for Forced Convection

4.2.3 3D Response Graphs for Forced Convection

The response of varying two input parameters and its effects on thermal resistance and pressure drop across the heatsink is generated using optiSLang

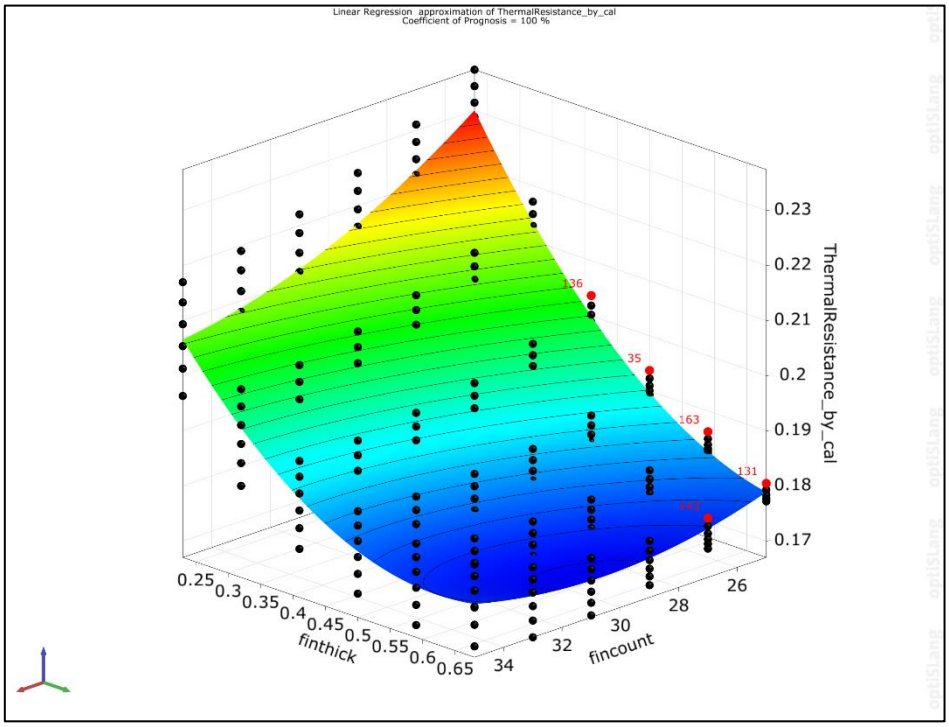

Figure 24 Surface Response for fin thickness and number of fins vs thermal resistance for Forced Convection

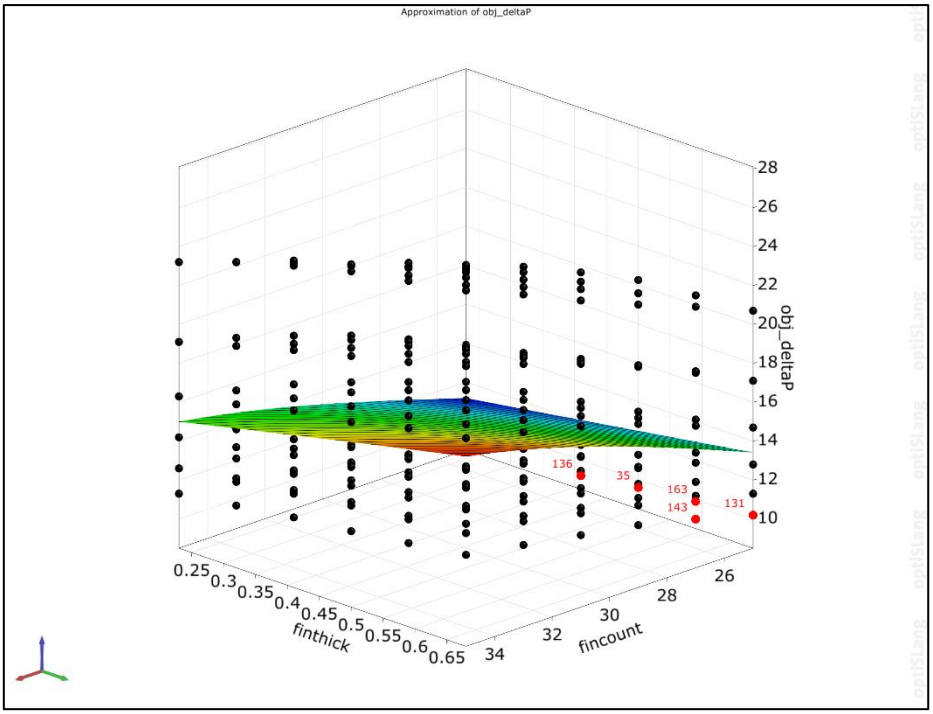

Figure 25 Surface Response for fin thickness and number of fins vs pressure drop for Forced Convection

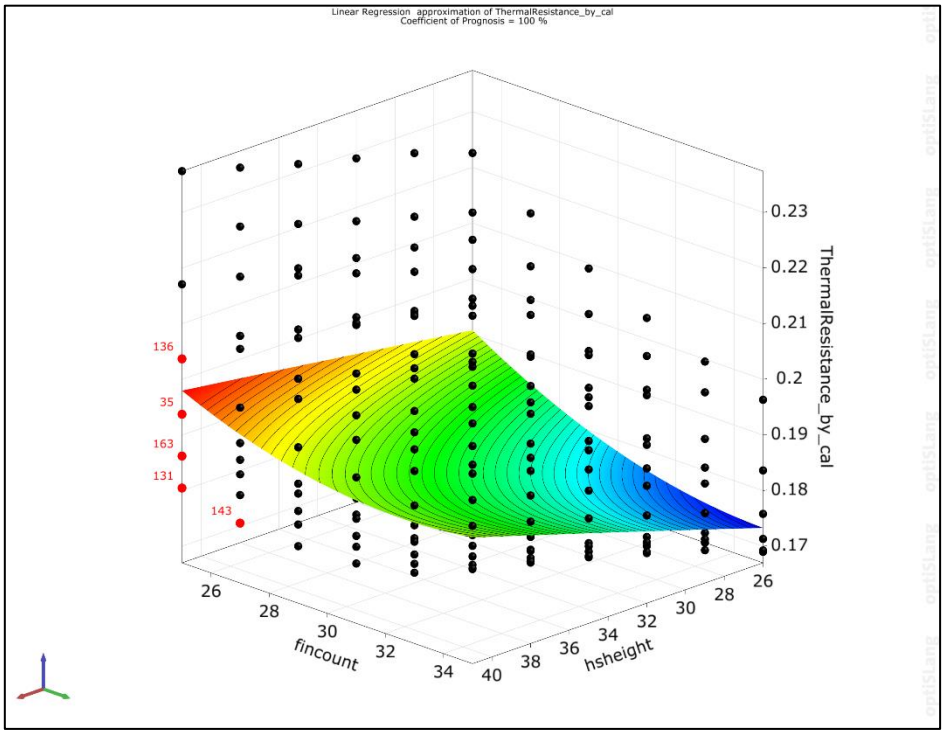

Figure 26 Surface Response for number of fins and heatsink height vs thermal resistance for Forced Convection

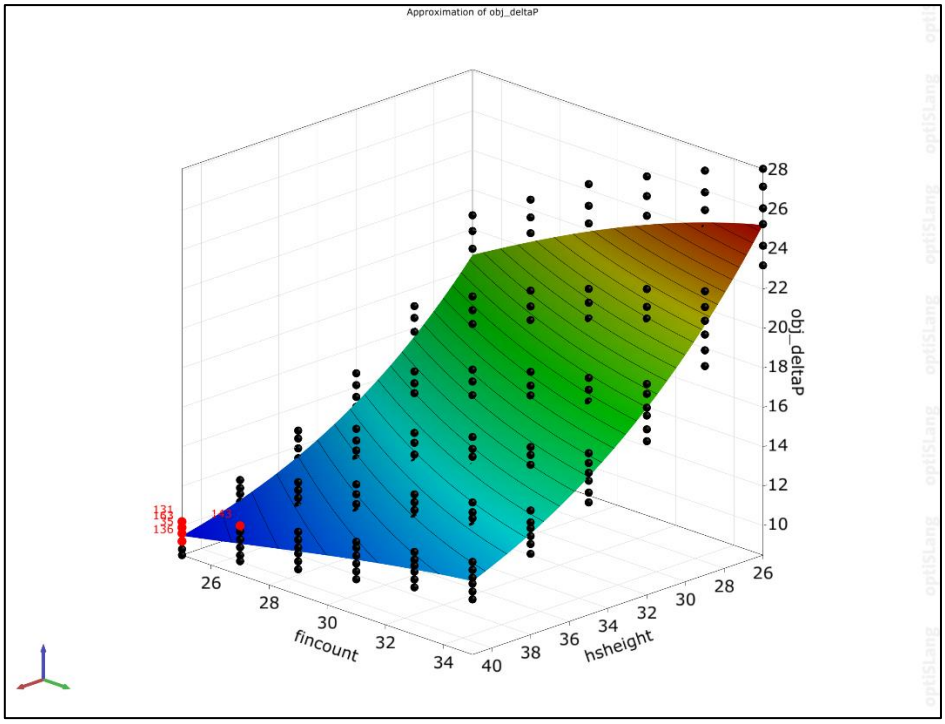

Figure 27 Surface Response for number of fins and heatsink height vs pressure drop for Forced Convection

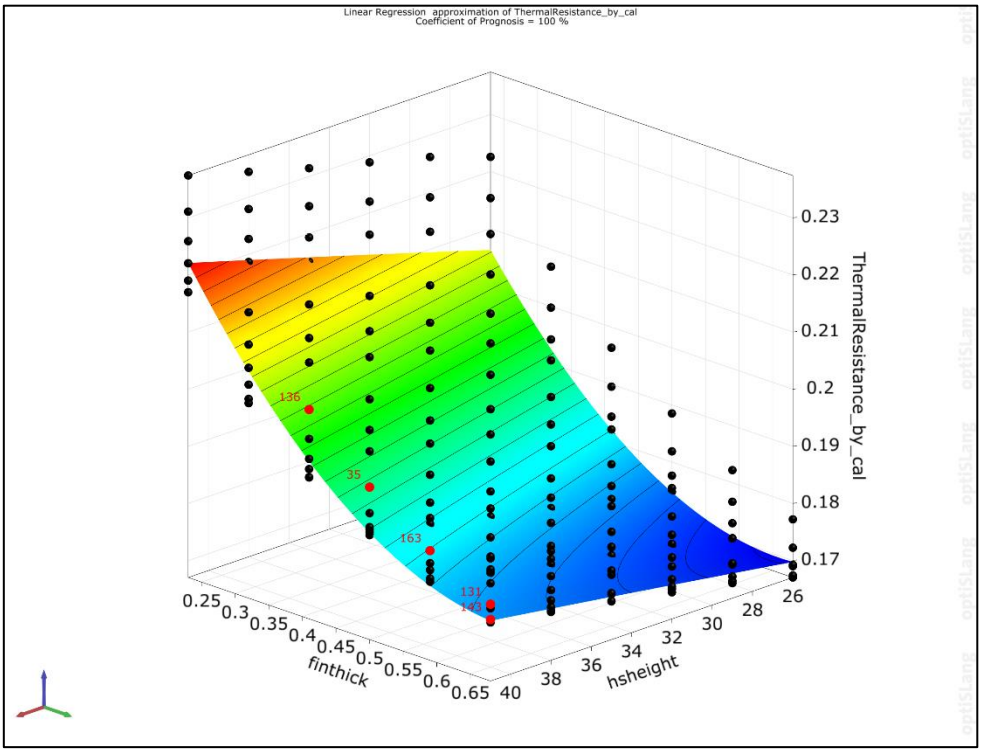

Figure 28 Surface Response for fin thickness and heatsink height vs thermal resistance for Forced Convection

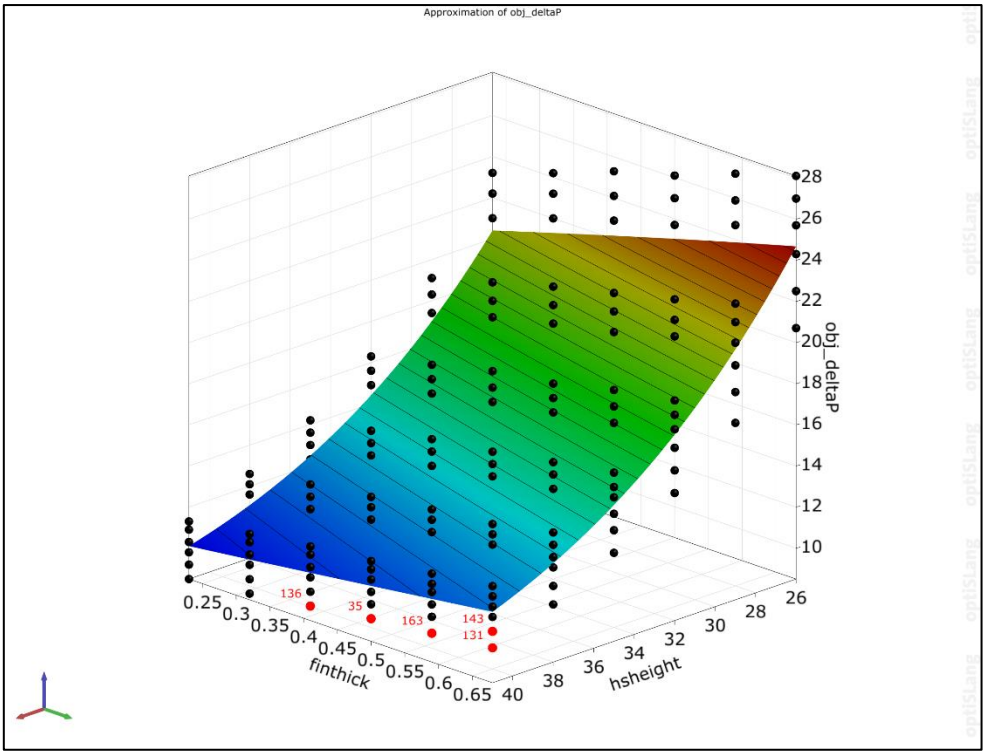

Figure 29 Surface Response for fin thickness and heatsink height vs pressure drop for Forced Convection

4.2.4 Best Design Point for Forced Convection for Aluminum Heatsink (2U)

optiSLang develops an Objective Pareto 2D graph with the two objectives, thermal resistance on x – axis and the pressure drop on y – axis. This graph provides us with the best design points amongst 216 design points.

The design points closer to the y – axis such as 208, 130, 148, 97, etc. have least thermal resistance but higher pressure drop. Whereas design points closer to x – axis like 35, 136, 96, 106 have least pressure drop but higher thermal resistance than the baseline model.

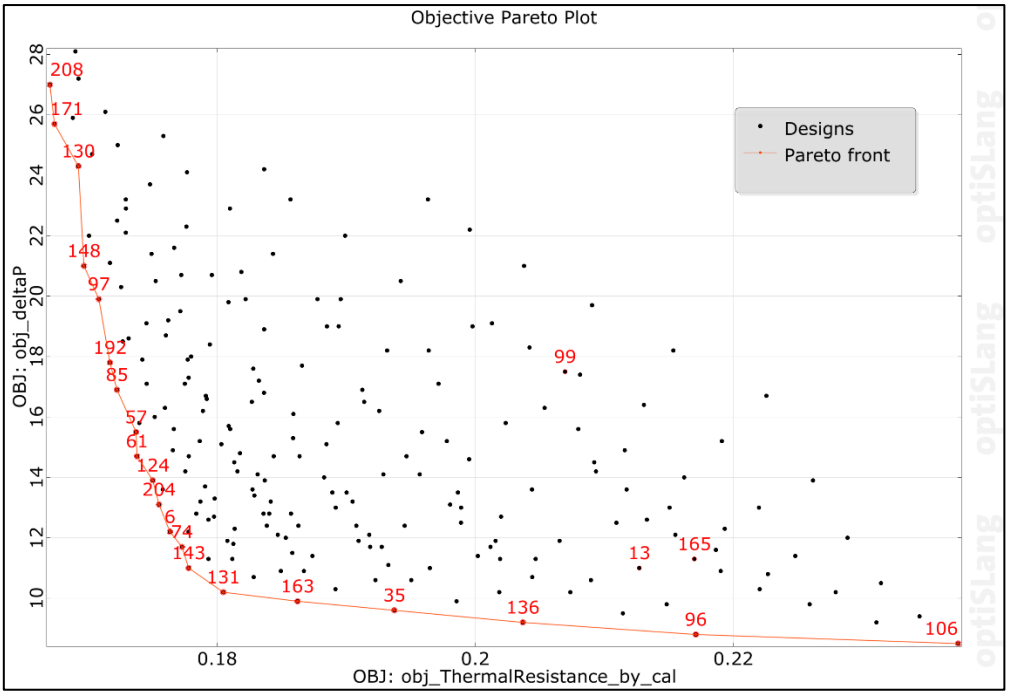

Figure 30 Pareto Graph for Forced Convection for Aluminum Heatsink

Hence, we select the design points in the gray zone closer to the origin such as 35, 131, 136, 143, 163.

Table 8 Design Points for Forced Convection for Aluminum Heatsink 2U

Design Point	Heatsink Height	Number of Fins	Heatsink Fin Thickness	Thermal Resistance	Pressure Drop	Heatsink Base Temperature	Source Temperature
Base Line	41	35	0.23	0.21698	11.3	54.9527	57.437
35	41	25	0.5	0.193725	9.6	52.2783	54.799
131	41	25	0.68	0.180473	10.2	50.7544	53.279
136	41	25	0.41	0.203687	9.2	53.424	55.931
143	41	27	0.68	0.177786	11	50.4453	52.933
163	41	25	0.59	0.186222	9.9	51.4153	53.939

Table 9 Best Design Point for Forced Convection for Aluminum Heatsink 2U

Design Point	Thermal Resistance	Percentage Change with Base Line	Pressure Drop	Percentage Change with Base Line	Base Temperature	Source Temperature
Base Line	0.21698		11.3		54.9527	57.437
35	0.19372	10.7199 %	9.6	15.044 %	52.2783	54.800
131	0.18047	16.8264 %	10.2	9.7345 %	50.7544	53.279
163	0.18622	14.1764%	9.9	12.9894 %	51.4153	53.939

Design point 35 has better efficiency with pressure drop whereas design point 131 has better efficiency with thermal resistance. But design point 163 stands between points 35 and 131 and tends to be optimum point for the optimization. Hence, we select design point 163 for 2U forced convection case for Aluminum heatsink.

Table 10 Optimized Aluminum Heatsink for Forced Convection 2U

Parameter	Baseline Heatsink (2U)	Optimized Heatsink (2U)
Material	Aluminum	Aluminum
Density	2710 kg/m^3	2710 kg/m^3
Specific Heat	896 J/kg – K	896 J/kg – K
Conductivity	220 W/m – K	220 W/m – K
Surface Area	305756 mm^2	224851 mm^2
Fin Separation	2.263 mm	2.927 mm

4.2.5 Best Design Point for Forced Convection for Aluminum Heatsink (1.5U)

With the same set of 216 design points, we can find the optimized heatsink for 1.5U servers. The logic behind this optimization is that same thermal resistance and pressure drop as that of baseline 2U server can be achieved with a heatsink for 1.5U server.

Table 11 Design Points for Forced Convection for Aluminum Heatsink 1.5U

Design Point	Heatsink Height	Number of Fins	Heatsink Fin Thickness	Thermal Resistance	Pressure Drop	Heatsink Base Temperature	Source Temperature
Base Line (2U)	41	35	0.23	0.21698	11.3	54.9527	57.437
161	35	25	0.41	0.20019	11.4	53.0219	55.552
13	35	25	0.32	0.21278	11	54.4697	56.9797
89	35	27	0.41	0.19458	12.4	52.3767	54.8541
206	35	35	0.68	0.17912	16.7	50.5986	53.082
179	35	35	0.23	0.20935	14.2	54.0752	56.5605

In the design point 13 has the same thermal resistance and pressure drop as that of the baseline 2U heatsink. Hence, this optimization is based upon form factor reduction from 2U to 1.5U heatsink.

4.2.6 Best Design Point for Forced Convection for Aluminum Heatsink (1U)

Table 12 Design Points for Forced Convection for Aluminum Heatsink 1U

Design Point	Heatsink Height	Number of Fins	Heatsink Fin Thickness	Thermal Resistance	Pressure Drop	Heatsink Base Temperature	Source Temperature
Base Line (2U)	41	35	0.23	0.21698	11.3	54.9527	57.437
120	26	35	0.68	0.16906	28.1	49.4419	51.9194
99	26	25	0.32	0.20695	17.5	53.7992	56.3044
41	26	27	0.23	0.21534	18.2	54.7641	57.2486
171	26	31	0.68	0.16739	25.7	49.2498	51.7346
24	26	33	0.41	0.17771	24.1	50.4366	56.5605

The design point 99 has the same thermal resistance with slight increase in pressure drop as compared to baseline heatsink of 2U server.

4.3 Results for Forced Convection Case using Copper Heatsink

With the same dimensions and boundary conditions for forced convection type of cooling, the Aluminum heatsink were replaced with the Copper heatsink with same geometry and variable set of input parameters. Copper heatsink were analyzed for forced convection.

4.3.1 Total Effects for Forced Convection for Copper Heatsink

Through the total effects chart generated using optiSLang it is depicted that pressure drop (deltaP) is majorly affected by heatsink height by 69.9 % and least affected by heatsink fin thickness by 6.5% whereas thermal resistance (ThermalResistance_by_cal) is majorly affected by heatsink fin thickness by 78.3% and least by heatsink height 4.8%

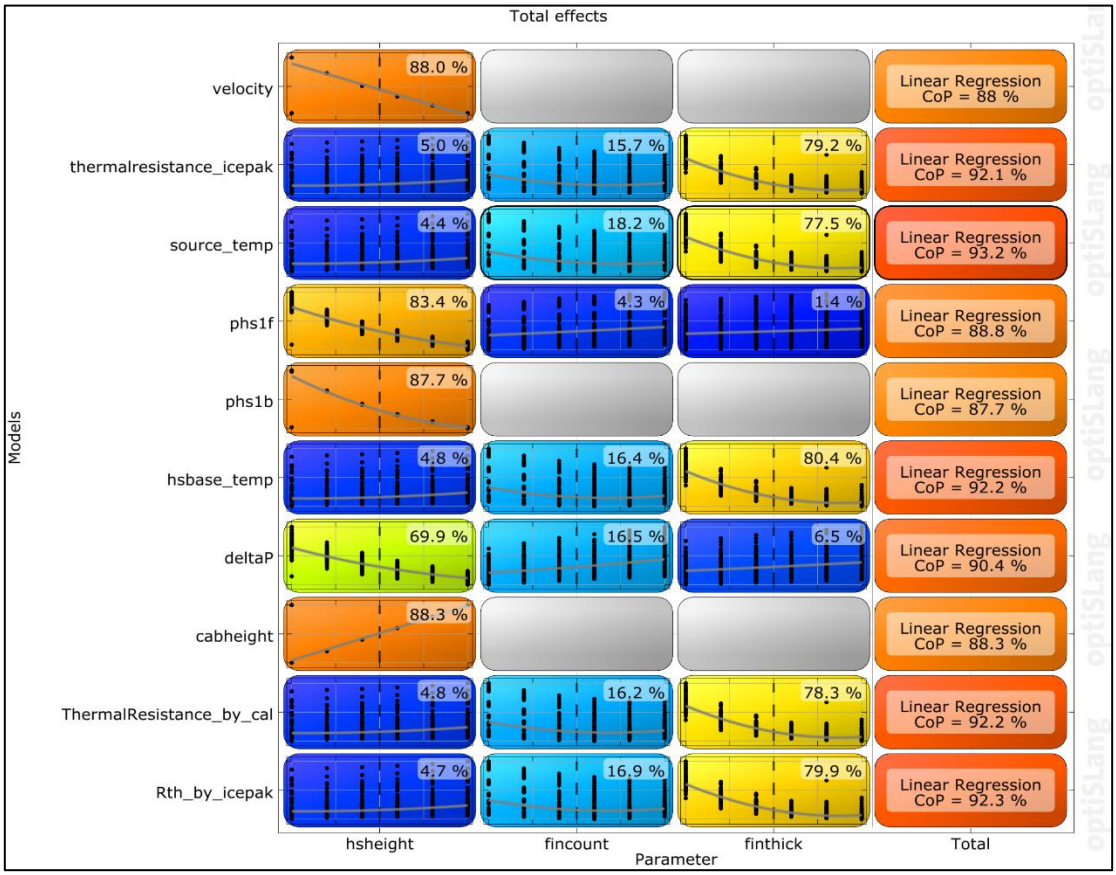

Figure 31 Total Effect for Forced Convection for Copper Heatsink

4.3.2 Best Design Point for Forced Convection for Copper Heatsink (2U)

The objective pareto plot explains the relationship between the two objectives and provides us with the best design points. The best design points from this objective pareto plot are selected and are; 27, 28, 158, 199, 207.

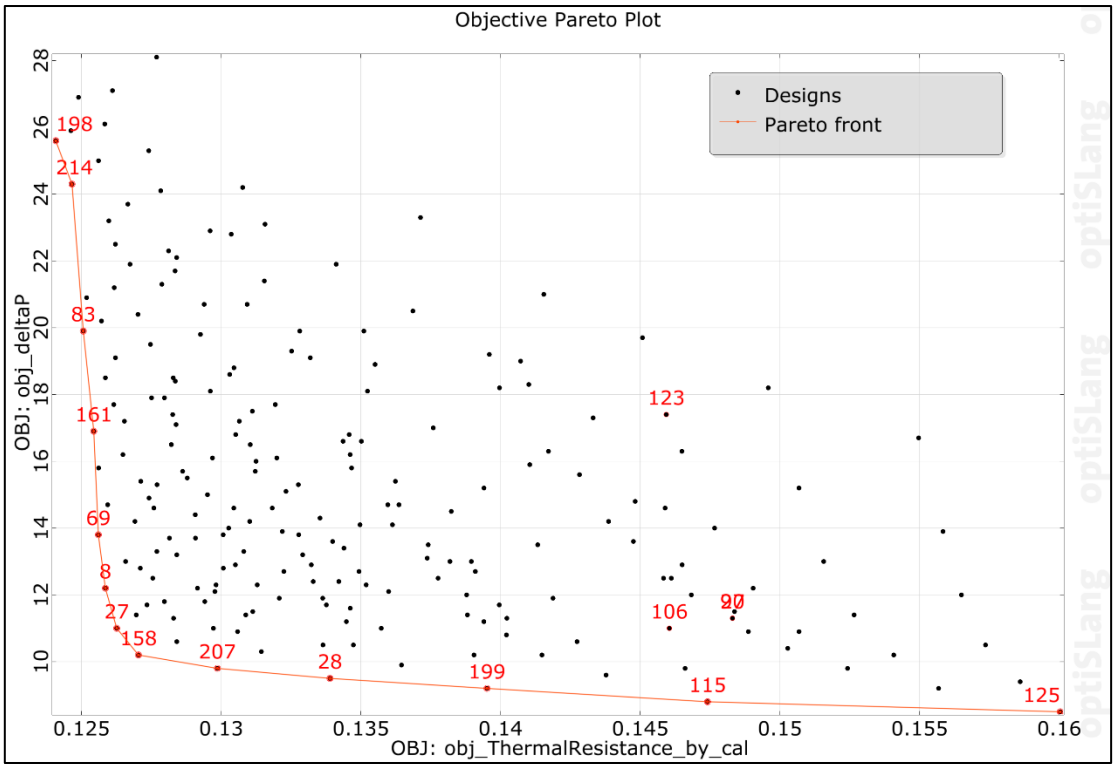

Figure 32 Pareto Graph for Forced Convection for Copper Heatsink

Table 13 Design Points for Forced Convection for Copper Heatsink 2U

Design Point	Heatsink Height	Number of Fins	Heatsink Fin Thickness	Thermal Resistance	Pressure Drop	Heatsink Base Temperature	Source Temperature
Base Line	41	35	0.23	0.14835	11.3	47.0602	49.622
27	41	27	0.68	0.12629	11.0	44.5233	47.252
28	41	25	0.5	0.13393	9.5	45.4019	48.172
158	41	25	0.41	0.13951	10.2	44.6096	47.384
199	41	27	0.68	0.13951	9.2	46.0436	48.813
207	41	25	0.59	0.12990	9.8	44.9385	47.709

Table 14 Best Design Points for Forced Convection for Copper Heatsink 2U

Design Point	Thermal Resistance	Percentage Change with Base Line	Pressure Drop	Percentage Change with Base Line	Heatsink Base Temperature	Source Temperature
Base Line	0.14835		11.3		47.0602	49.622
28	0.13389	9.7472 %	9.5	15.9292 %	45.3973	48.172
158	0.12704	14.3647 %	10.2	9.7345 %	44.6096	47.384
207	0.12986	12.4638 %	9.8	13.2743 %	44.9339	47.709

Design point 28 has better efficiency with pressure drop whereas design point 158 has better efficiency with thermal resistance. But design point 207 stands between points 28 and 158 and tends to be optimum design point for the optimization. Hence, we select design point 207 for 2U forced convection case for Copper heatsink.

Table 15 Optimized Copper Heatsink for Forced Convection 2U

Parameter	Baseline Heatsink (2U)	Optimized Heatsink (2U)
Material	Copper	Copper
Density	8950 kg/m^3	8950 kg/m^3
Specific Heat	380 J/kg – K	380 J/kg – K
Conductivity	386 W/m – K	386 W/m – K
Surface Area	305756 mm^2	224851 mm^2
Fin Separation	2.263 mm	2.927 mm

4.3.3 Best Design Point for Forced Convection for Copper Heatsink (1.5U)

With the same set of 216 design points, we found the optimized heatsink for 1.5U servers. The logic behind this optimization is that same thermal resistance and pressure drop as that of baseline 2U server can be achieved with a heatsink for 1.5U server.

Table 16 Best Design Points for Forced Convection for Copper Heatsink 1.5U

Design Point	Heatsink Height	Number of Fins	Heatsink Fin Thickness	Thermal Resistance	Pressure Drop	Heatsink Base Temperature	Source Temperature
Base Line (2U)	41	35	0.23	0.14835	11.3	47.0602	49.622
106	35	25	0.32	0.4608	11	46.7992	49.5624
215	35	25	0.23	0.15741	10.5	48.1021	50.855
210	35	35	0.59	0.13199	16.1	45.1788	47.739
132	35	27	0.23	0.15271	11.4	47.5616	50.2917

In the design point 106 has the same thermal resistance and pressure drop as that of the baseline 2U heatsink. Hence, this optimization is based upon form factor reduction from 2U to 1.5U heatsink.

4.3.4 Best Design Point for Forced Convection for Copper Heatsink (1U)

Table 17 Best Design Points for Forced Convection for Copper Heatsink 1U

Design Point	Heatsink Height	Number of Fins	Heatsink Fin Thickness	Thermal Resistance	Pressure Drop	Heatsink Base Temperature	Source Temperature
Base Line (2U)	41	35	0.23	0.14835	11.3	47.0602	49.622
20	26	25	0.59	0.14835	11.3	47.0602	49.622
38	26	35	0.68	0.12773	28.1	44.6889	47.247
123	26	25	0.32	0.14592	16.2	46.7822	49.528
188	26	33	0.23	0.14435	11.5	46.6002	49.723
60	26	31	0.32	0.14621	11.4	46.8141	49.802

The design point 20 has the same thermal resistance and pressure drop as compared to baseline heatsink of 2U server. Hence, we can cool the same amount of TDP of a 2U server heatsink using 1U server heatsink.

4.4 Results for Natural Convection Case using Aluminum Heatsink

The same 216 design points were used to find an optimized Aluminum heatsink for natural convection cooling of server. The fluid temperature, TDP for each CPU, Heatsink Base Area, Heatsink Base Height were kept constant whereas heatsink fin thickness, heatsink fin height and number of fins were varied as mentioned in table. The boundary conditions for natural convection are explained in section 3.9

4.4.1 Total Effects for Natural Convection for Aluminum Heatsink

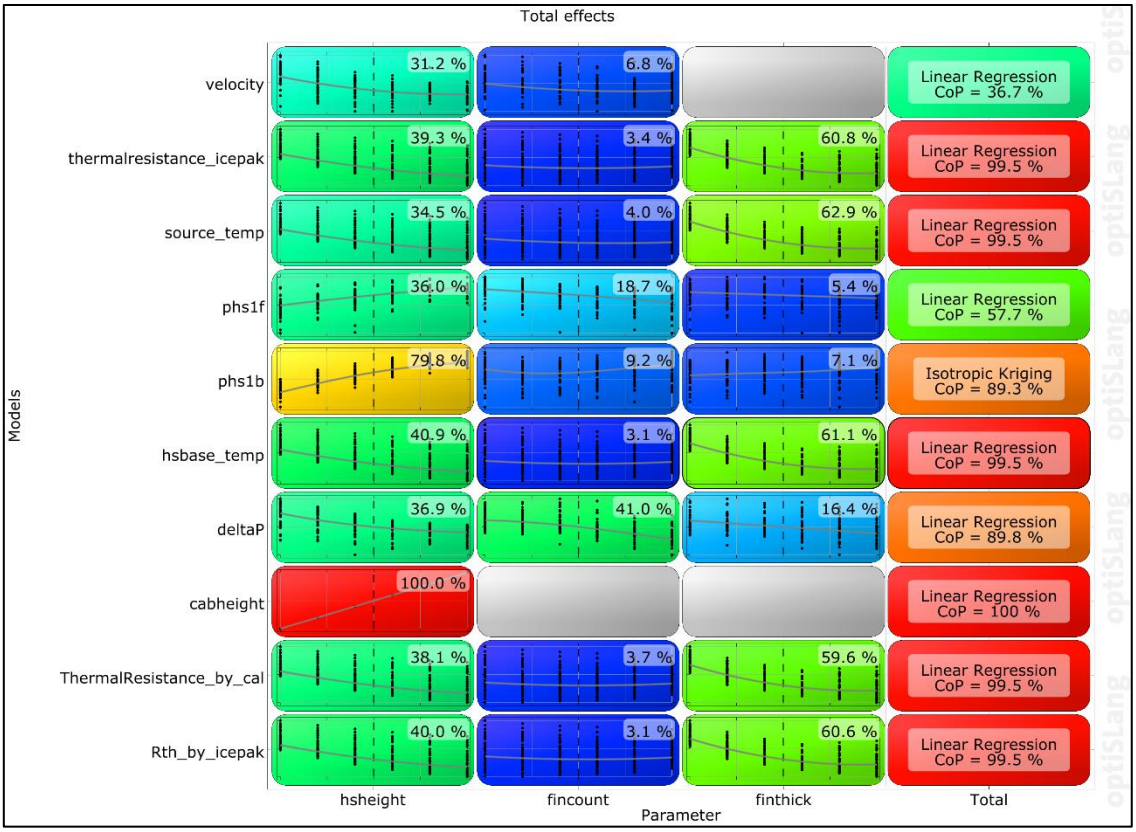

Figure 33 Total Effect for Natural Convection for Aluminum Heatsink

The total effects chart denotes that objective pressure drop (deltaP) is majorly affected by heatsink number of fins - 41.0 % and heatsink fin height - 36.9 % and least affected by heatsink fin thickness - 16.4 %. Whereas, the other objective thermal resistance

(ThermalResistance_by_cal) is majorly affected by heatsink fin thickness - 59.6 % followed by heatsink fin height - 38.1 % and least by heatsink number of fins - 3.7 %.

4.4.2 Response graphs for Natural Convection

The response graphs of the two objectives namely thermal resistance and pressure drop against the three varying input parameters are generated. The thermal resistance decreases with increase in heatsink fin thickness and heatsink fin height whereas it increases with increase in heatsink number of fins.

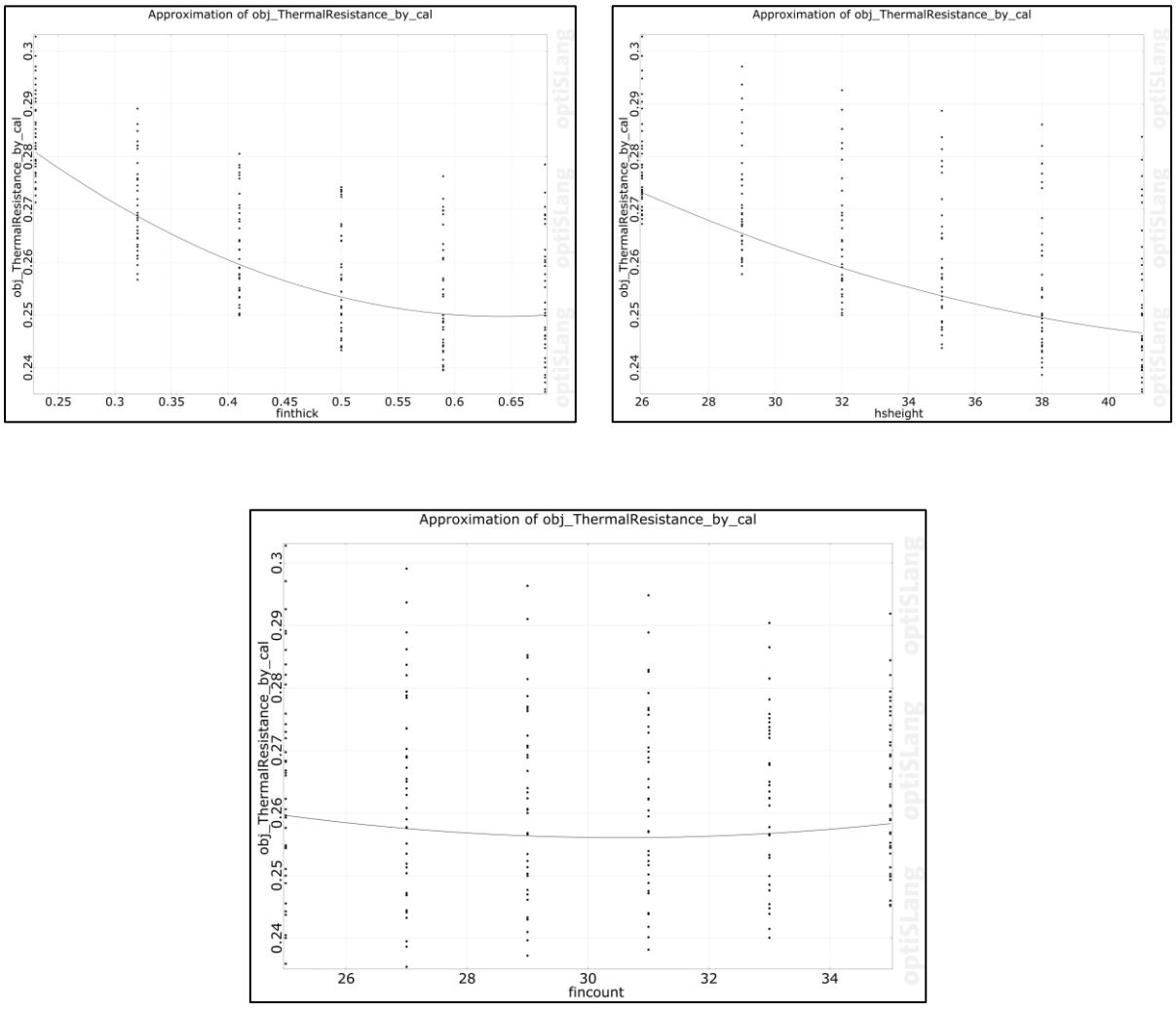

Figure 34 Response Curves for Thermal Resistance for Natural Convection

The pressure drop across the heatsink in natural convection decreases with increase in heatsink fin height and heatsink number of fins it decreases sightly increase in heatsink fin thickness.

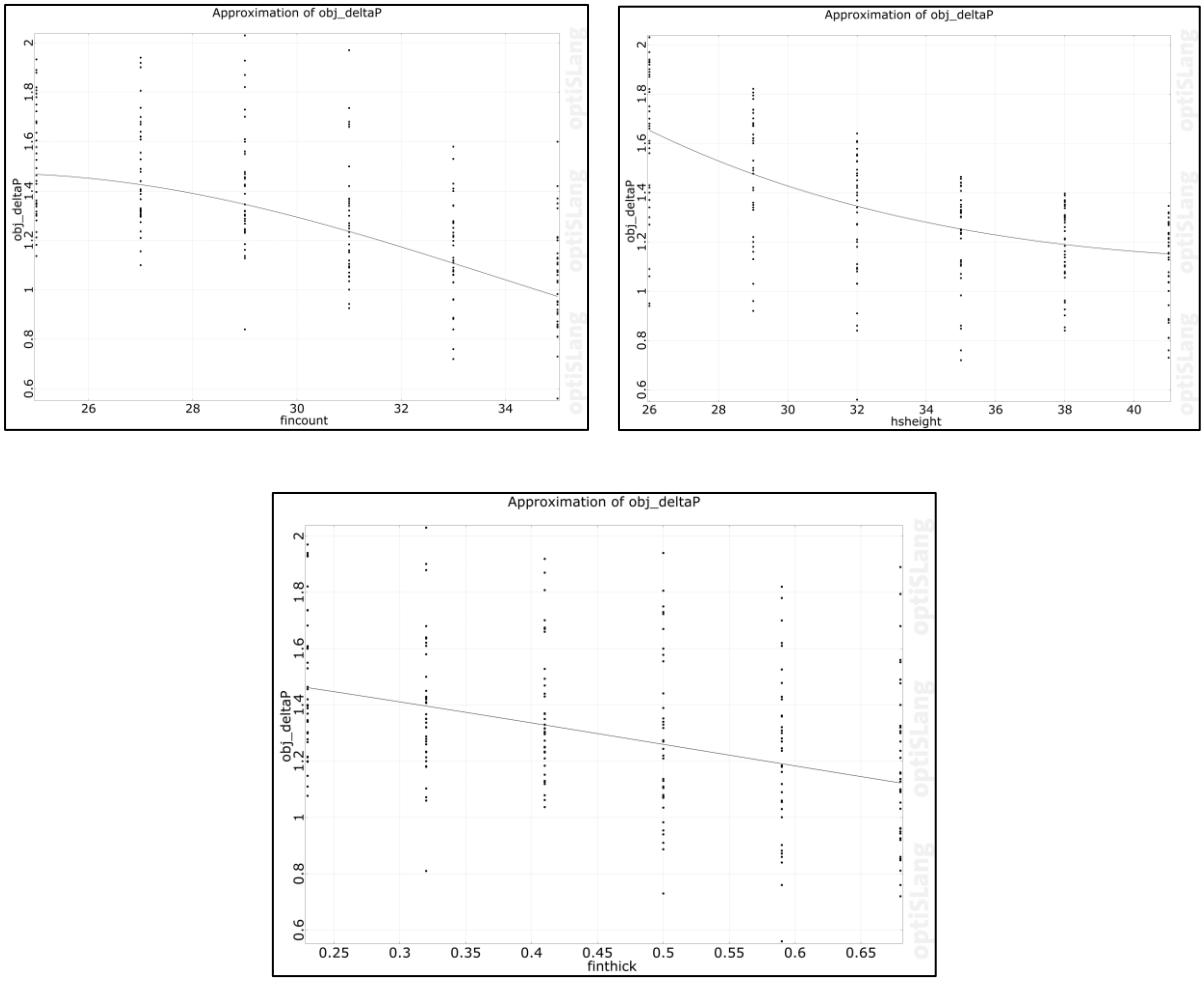

Figure 35 Response Curves for Pressure Drop for Natural Convection

4.4.3 3D Response Graphs for Natural Convection

The response of varying two input parameters and its effects on thermal resistance and pressure drop across the heatsink for Natural Convection cooling of servers is generated using optiSLang

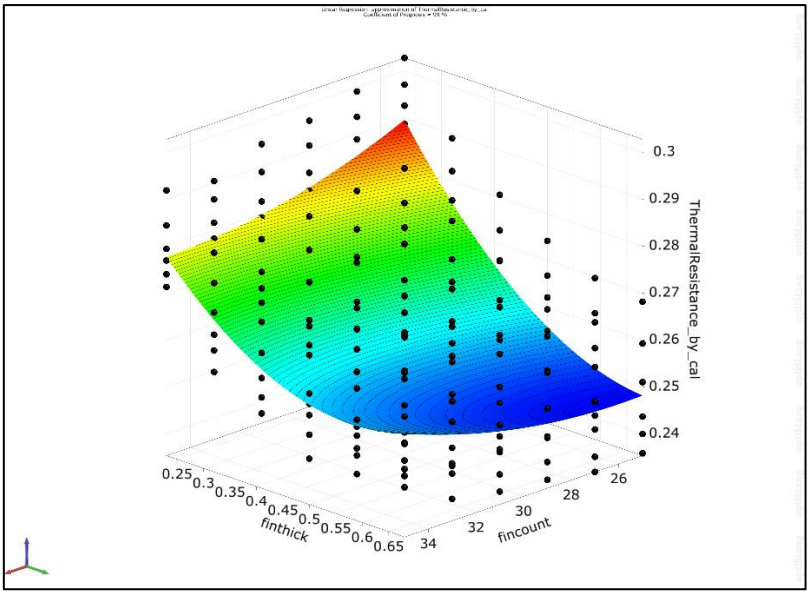

Figure 36 Surface Response for fin thickness and number of fins vs thermal resistance for Natural Convection

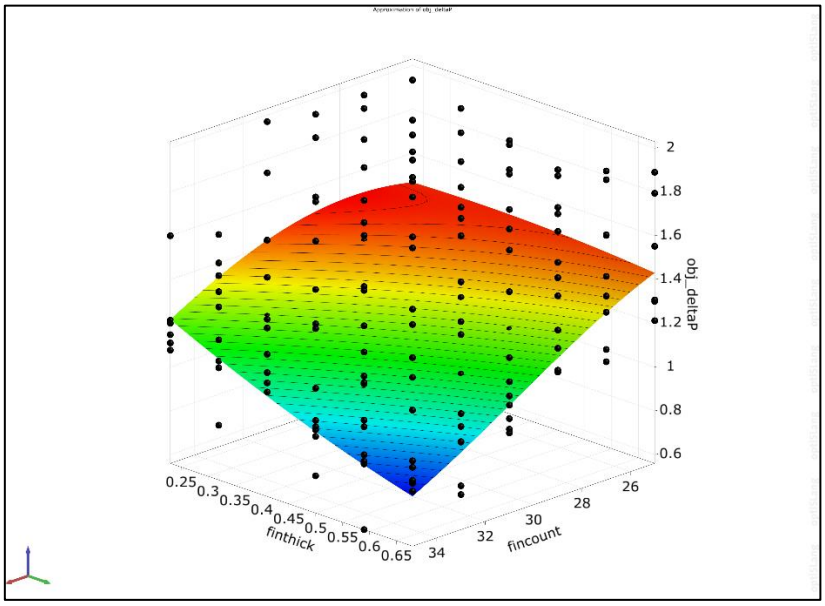

Figure 37 Surface Response for fin thickness and number of fins vs pressure drop for Natural Convection

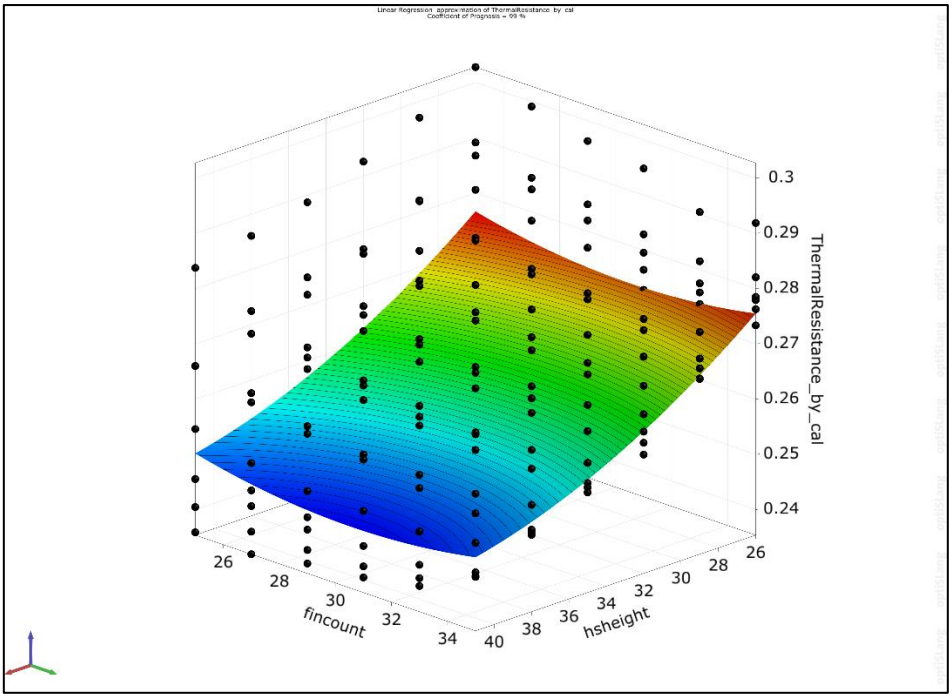

Figure 38 Surface Response for number of fins and heatsink height vs thermal resistance for Natural Convection

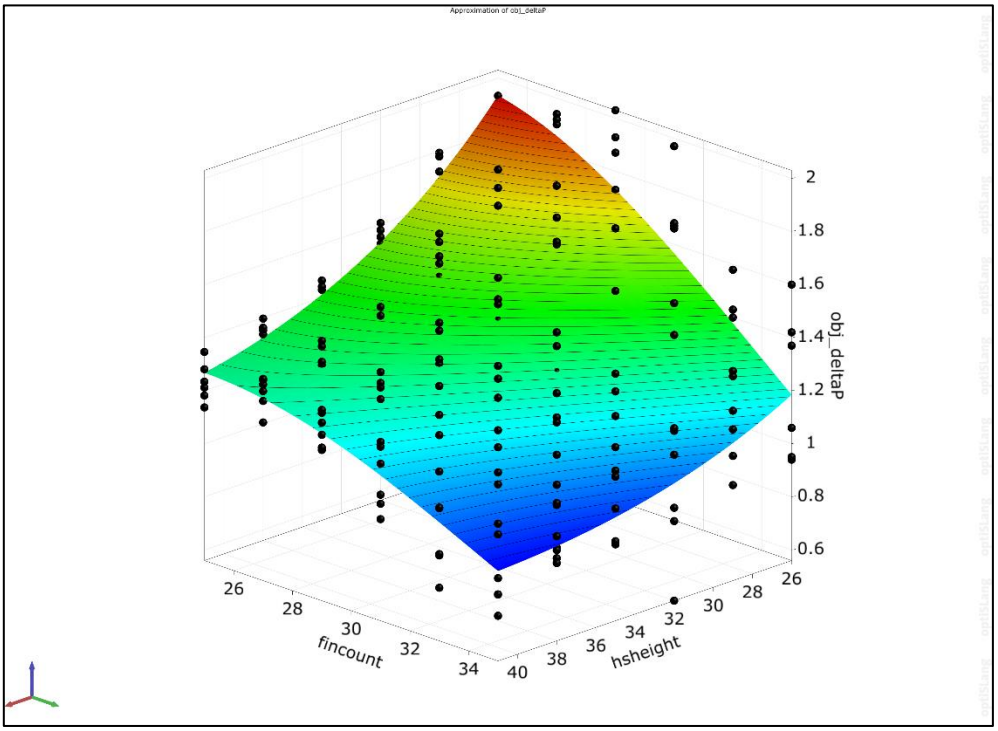

Figure 39 Surface Response for number of fins and heatsink height vs pressure drop for Natural Convection

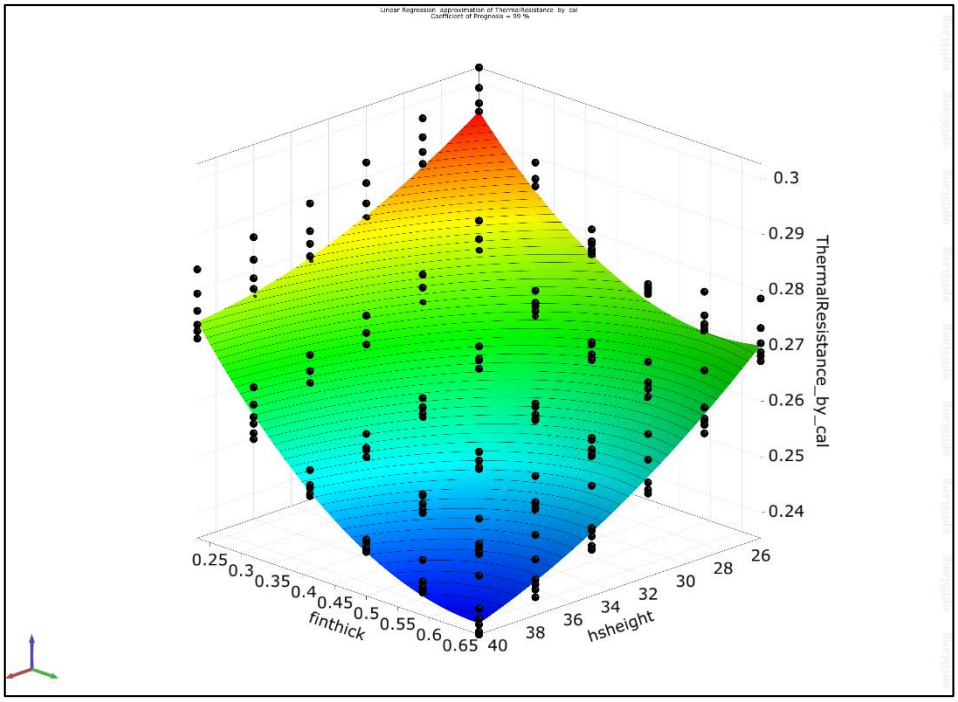

Figure 40 Surface Response for fin thickness and heatsink height vs thermal resistance for Natural Convection

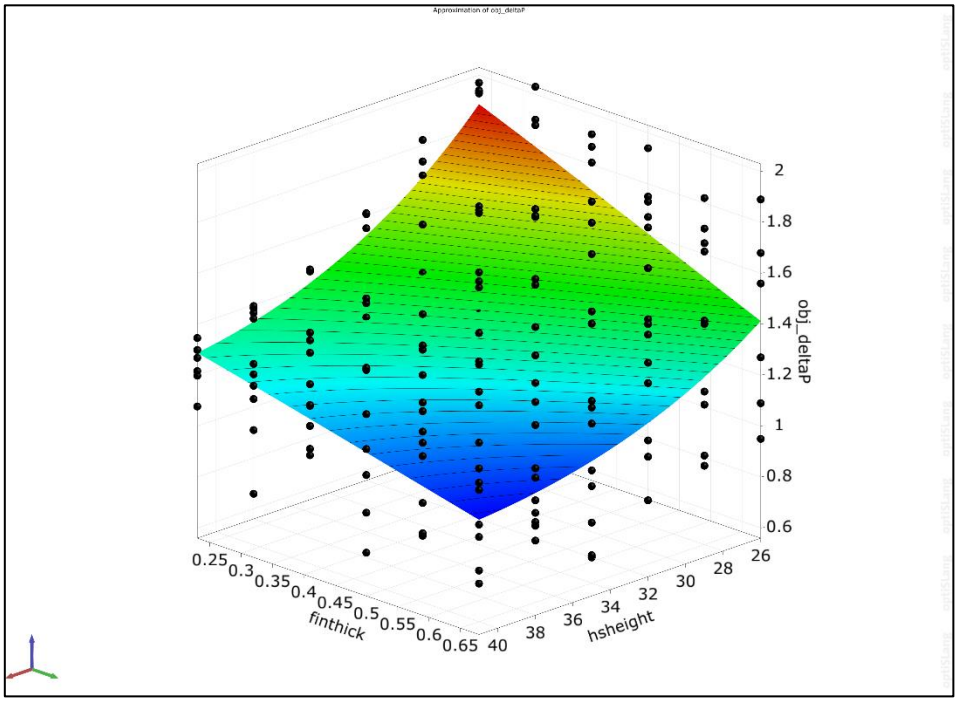

Figure 41 Surface Response for fin thickness and heatsink height vs pressure drop for Natural Convection

4.4.4 Best Design Point for Natural Convection for Aluminum Heatsink (2U)

The objective pareto plot explains the relationship between the thermal resistance and pressure drop and provides us with the best design points. The best design points from this objective pareto plot are selected and are; 100, 201, and 132.

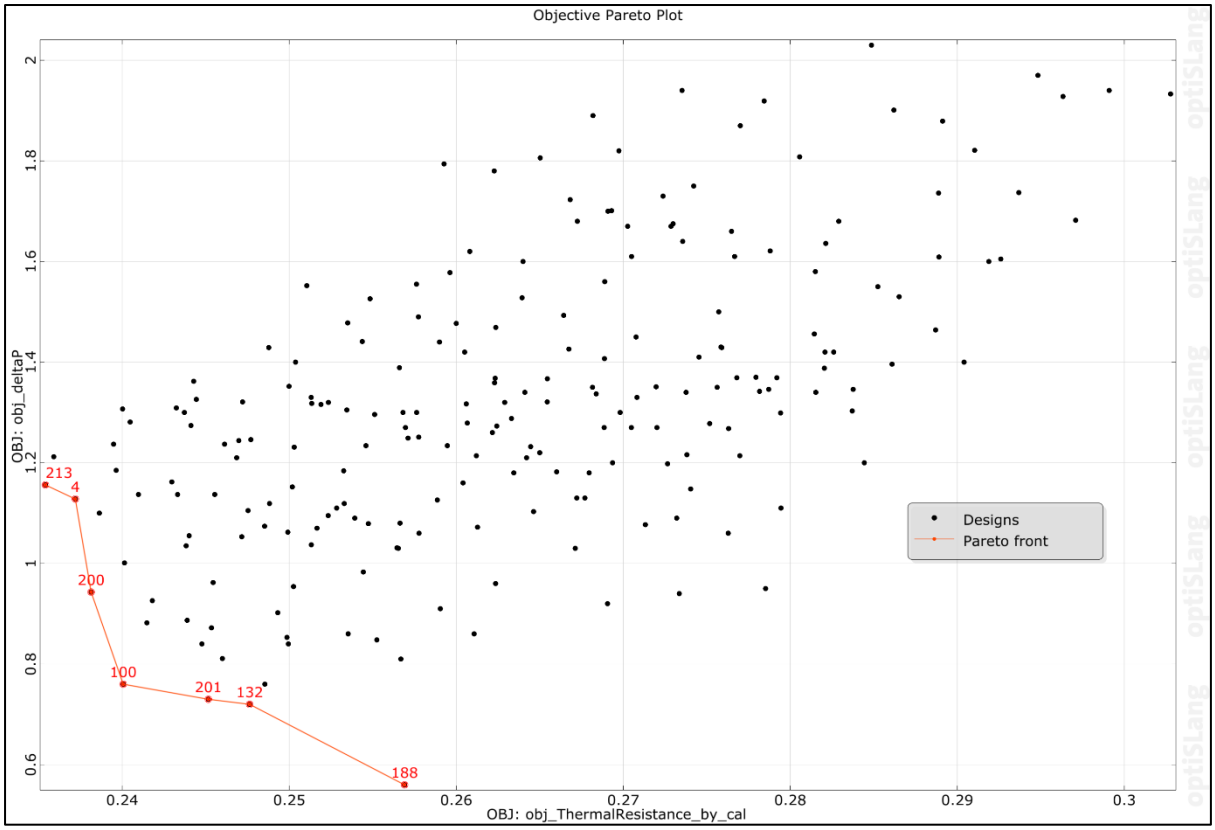

Figure 42 Pareto Graph for Natural Convection for Aluminum Heatsink

Table 18 Design Points for Natural Convection for Aluminum Heatsink 2U

Design Point	Heatsink Height	Number of Fins	Heatsink Fin Thickness	Thermal Resistance	Pressure Drop	Heatsink Base Temperature	Source Temperature
Base Line	41	35	0.23	0.27132	1.077	61.2018	64.173
100	41	33	0.68	0.20406	0.76	57.6066	60.4432
132	41	33	0.68	0.24763	0.72	58.4773	61.2820
201	41	35	0.5	0.24516	0.73	58.1932	61.0281

Table 19 Best Design Points for Natural Convection for Aluminum Heatsink 2U

Design Point	Thermal Resistance	Percentage Change with Base Line	Pressure Drop	Percentage Change with Base Line	Heatsink Base Temperature	Source Temperature
Base Line	0.27132		1.077		61.2018	64.173
100	0.20406	11.5222 %	0.76	29.4336 %	45.3973	48.172
132	0.24763	8.7318 %	0.72	33.1476 %	44.6096	47.384
201	0.24516	9.6421 %	0.73	32.2191 %	44.9339	47.709

The design point 100 has better reduction in thermal resistance as compared to baseline model whereas design point 132 has better reduction in pressure drop whereas design point 201 has significant reduction in both thermal resistance and pressure drop. Hence, we say heatsink with design point 201 parameters is the optimized heatsink for natural convection for Aluminum heatsink for 2U server.

Table 20 Optimized Aluminum Heatsink for Natural Convection 2U

Parameter	Baseline Heatsink (2U)	Optimized Heatsink (2U)
Material	Aluminum	Aluminum
Density	2710 kg/m^3	2710 kg/m^3
Specific Heat	896 J/kg – K	896 J/kg – K
Conductivity	220 W/m – K	220 W/m – K
Surface Area	305756 mm^2	306455 mm^2
Fin Separation	2.263 mm	1.985 mm

4.4.5 Best Design Point for Natural Convection for Aluminum Heatsink (1.5U)

With 216 design points, we found heatsink parameters for optimized heatsink for 1.5U servers.

Table 21 Design Points for Natural Convection for Aluminum Heatsink 1.5U

Design Point	Heatsink Height	Number of Fins	Heatsink Fin Thickness	Thermal Resistance	Pressure Drop	Heatsink Base Temperature	Source Temperature
Base Line (2U)	41	35	0.23	0.27132	1.077	61.2018	64.173
63	35	35	0.5	0.25453	0.983	59.2709	62.0557
132	35	33	0.68	0.24772	0.72	58.4878	61.28220
155	35	33	0.59	0.24863	0.76	58.5925	61.4121
198	35	31	0.5	0.25175	1.07	58.9512	61.8838

In the design point 132 has significant reduction in pressure drop and thermal resistance as that of the baseline 2U heatsink. Hence, this optimization is based upon form factor reduction from 2U to 1.5U heatsink.

4.4.6 Best Design Point for Natural Convection for Aluminum Heatsink (1U)

Table 22 Best Design Points for Natural Convection for Aluminum Heatsink 1U

Design Point	Heatsink Height	Number of Fins	Heatsink Fin Thickness	Thermal Resistance	Pressure Drop	Heatsink Base Temperature	Source Temperature
Base Line (2U)	41	35	0.23	0.27132	1.077	61.2018	64.173
24	26	25	0.68	0.26829	1.89	60.8533	63.8272
107	26	27	0.68	0.26736	1.68	60.7464	63.6476
110	26	35	0.5	0.27347	0.94	61.4491	64.1123
148	26	33	0.68	0.27332	1.09	61.4318	64.0675

The design point 110 has the same thermal resistance and reduced pressure drop as compared to baseline heatsink of 2U server. Hence, we the heatsink having parameters of design point 110 can cool the same amount of TDP of a 2U server heatsink using 1U server heatsink.

4.5 Results for Natural Convection Case using Copper Heatsink

With the same dimensions and boundary conditions for natural convection type of cooling, the Aluminum heatsink were replaced with the Copper heatsink with same geometry and variable set of input parameters. Copper heatsink were analyzed for natural convection.

4.5.1 Total Effects for Natural Convection for Copper Heatsink

Using the total effects chart generated using optiSLang it is depicted that pressure drop (deltaP) is majorly affected by heatsink number of fins by 36.9 % and by heatsink fin height by 36.3 % whereas thermal resistance (ThermalResistance_by_cal) is majorly affected by heatsink fin height by 78.0 % and least by heatsink number of fins 7.9%

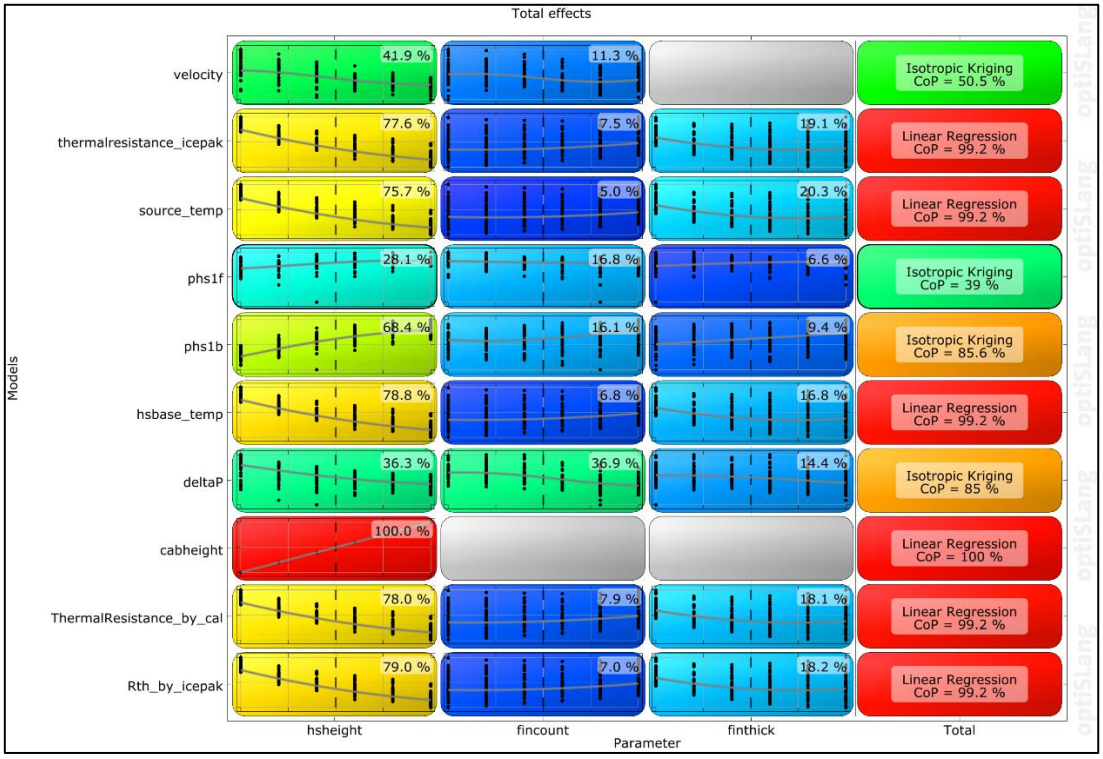

Figure 43 Total Effect for Natural Convection for Copper Heatsink

4.5.2 Best Design Point for Natural Convection for Copper Heatsink (2U)

Objective Pareto graph conveys that design points 29, 59, 193, and 196 are the best design points for natural convection for Copper Heatsink for (2U)

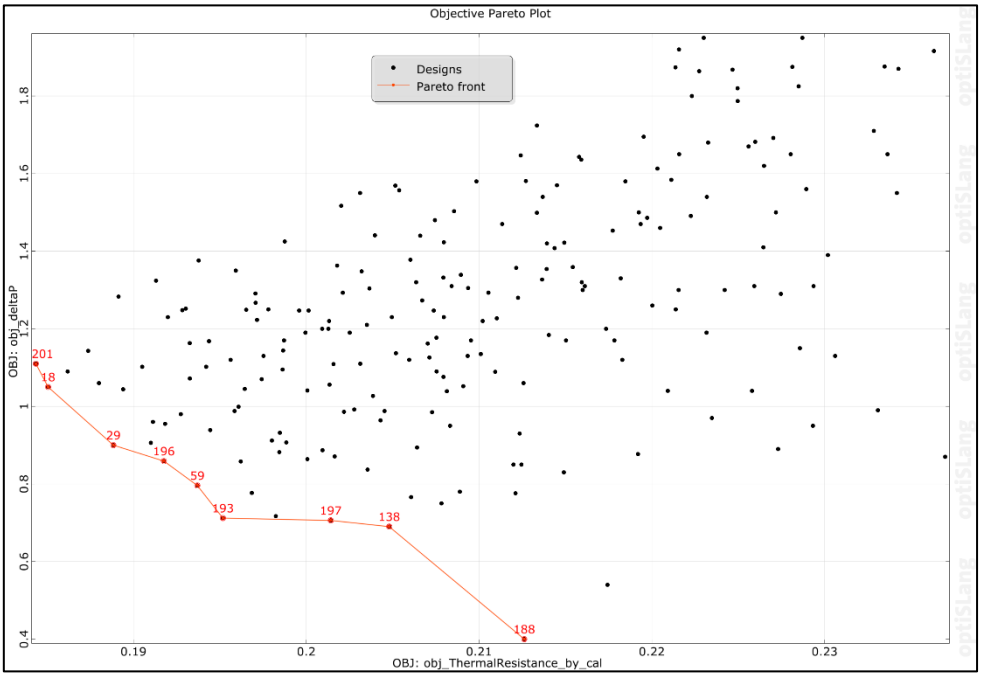

Figure 44 Pareto Graph for Natural Convection for Copper Heatsink

4.5.3 Best Design Point for Natural Convection for Copper Heatsink (2U)

The objective pareto plot explains the relationship between the two objectives pressure drop vs thermal resistance and provides us with the best design points. The best design points from this objective pareto plot are selected and are; 29, 59, 193, and 196.

Table 23 Design Points for Natural Convection for Copper Heatsink 2U

Design Point	Heatsink Height	Number of Fins	Heatsink Fin Thickness	Thermal Resistance	Pressure Drop	Heatsink Base Temperature	Source Temperature
Base Line	41	35	0.23	0.20728	0.985	53.8372	56.814
29	41	29	0.5	0.18884	0.9	51.7166	51.7166
59	41	33	0.59	0.19370	0.796	52.2755	52.2753
193	41	33	0.68	0.19518	0.712	52.2755	52.4455
196	41	31	0.68	0.19176	0.859	52.0524	52.0527

Table 24 Best Design Points for Natural Convection for Copper Heatsink 2U

Design Point	Thermal Resistance	Percentage Change with Base Line	Pressure Drop	Percentage Change with Base Line	Heatsink Base Temperature	Source Temperature
Base Line	0.20728		0.985		53.8372	56.814
29	0.18884	8.8962 %	0.9	8.6294 %	51.7166	51.7166
59	0.19370	6.5515 %	0.796	19.1878 %	52.2755	52.2753
193	0.19518	5.8375 %	0.712	27.7157 %	52.2755	52.4455
196	0.19176	7.4875 %	0.859	12.7919 &	52.0524	52.0527

The design point 59 has significant improvement in pressure drop and thermal resistance with the baseline model hence we select the heatsink parameters from design point 59 for natural convection cooling of server (2U) for Copper heatsink.

Table 25 Optimized Copper Heatsink 2U for Natural Convection

Parameter	Baseline Heatsink (2U)	Optimized Heatsink (2U)
Material	Copper	Copper
Density	8950 kg/m^3	8950 kg/m^3
Specific Heat	380 J/kg – K	380 J/kg – K
Conductivity	386 W/m – K	386 W/m – K
Surface Area	305756 mm^2	290321 mm^2
Fin Separation	2.263 mm	2.048 mm

4.5.4 Best Design Point for Natural Convection for Copper Heatsink (1.5U)

We found the optimized heatsink parameters for 1.5U servers. Same thermal resistance and pressure drop as that of baseline 2U server can be achieved with a heatsink for 1.5U server.

Table 26 Best Design Point for Natural Convection for Copper Heatsink 1.5U

Design Point	Heatsink Height	Number of Fins	Heatsink Fin Thickness	Thermal Resistance	Pressure Drop	Heatsink Base Temperature	Source Temperature
Base Line (2U)	41	35	0.23	0.21698	0.985	54.9527	57.437
63	35	25	0.68	0.19281	0.98	53.9096	55.2491
124	35	35	0.59	0.20791	0.75	53.9096	56.7559
136	35	33	0.59	0.20437	0.964	53.5025	56.394
138	35	23	0.68	0.20488	0.69	53.5612	56.4438

In the design point 138 has the same thermal resistance and pressure drop as that of the baseline 2U heatsink. Hence, this optimization is based upon reduction of form factor from 2U to 1.5U server heatsink.

Chapter 5 Conclusion and Future Work

Single-phase immersion cooling of servers using forced convection and natural convection has been studied and researched previously. Single-phase immersion cooling has proved more efficient than air cooling of data centers. In addition to being more efficient than air cooling, many moving parts such as fans are obsolete in immersion cooling. The servers are cut-off from the external environment and air contamination as seen in air cooling is completely taken aback. Hence, the reliability issues in immersion cooling are lesser. The power density of the data centers can be increased by reducing the form factor of server using immersion cooling techniques.

In this work, the effect of variable heatsink geometry parameters on the thermal resistance and pressure drop across the heatsink was studied for Aluminum and Copper heatsinks. It was understood that lesser thermal resistance was achieved by increase the surface area of the heatsink whereas lesser pressure drop was generated by reducing the heatsink fin thickness and increasing the heatsink height this was primarily due to hydraulic diameter and the volumetric flow rate set at 2 LPM for the forced convection case study. It is found that heatsink and pressure drop a heatsink are inversely proportional to each other depending upon the varying heatsink geometry parameters studied in this report. For forced convection cooling of 2U servers using Aluminum heatsink improvement of 14.1764 % in thermal resistance and 12.9894 % in pressure drop against the base line 2U server model. Whereas, we found optimized heatsinks for 1.5U and 1U server that can cool the same amount of TDP as that of a 2U server and same pressure drop for forced convection cooling using Aluminum and Copper heatsinks. In this work, single-phase immersion cooling using natural convection was studied as well. It was found that similar TDP of 2U server can be cooled by using heatsinks for 1.5U and 1U servers using Aluminum and Copper heatsinks.

In the future work for this study, experimental setup with the same boundary conditions of forced and natural convection must be studied and the results of this computational study must be verified by manufacturing heatsinks for 2U, 1.5U and 1U servers of the optimum design points generated in this study. Rigorous optimization of heatsinks with reduced step size in varying heatsink geometry parameters must be done using optiSLang to generate highly optimized heatsink. Optimization of heatsink depending upon the surface area and height of base of heatsink must be done and its effects must be understood. optiSLang must be used to optimize heatsinks for varying TDP, at different volumetric flow rates and varying inlet fluid temperatures. The reliability of single-phase immersion cooling can be understood using the experimental setup designed from this computational study. Optimization for 2-phase immersion cooling using dielectric fluid can be done using optiSLang [31]. Change in properties of the printed circuit board (PCBs) with temperature play a significant role on the reliability of the electronic packages [32]. Researchers are increasingly interested in improving the efficiency and reliability of immersion cooled components such as PCBs [33-35]. When assessing the qualities of materials, measurement techniques are a crucial issue to consider.

References

[1] T. Gao, H. Tang, Y. Cui and Z. Luo, "A Test Study of Technology Cooling Loop in a Liquid Cooling System," 2018 17th IEEE Intersociety Conference on Thermal and Thermomechanical Phenomena in Electronic Systems (ITherm), 2018, pp. 740-747, doi: 10.1109/ITHERM.2018.8419519.

[2] Iyengar, M., 2010, "Energy Consumption of Information Technology Data Centers,"

J. Electron. Cool., 16(4), epub.

[3] Andy Lawrence, April 2020, "Data center PUEs flat since 2013", Accessed January 7, 2020, Global Uptime Institute Survey, https://journal.uptimeinstitute.com/data-center-pues-flat-since-2013/

[4] Hoang, C.H., Khalili, S., Ramakrisnan, B., Rangarajan, S., Hadad, Y., Radmard, V., Sikka, K., Schiffres, S. and Sammakia, B., 2020, "An Experimental Apparatus for Two-phase Cooling of High Heat Flux Application using an Impinging Cold Plate and Dielectric Coolant," *36th Semiconductor Thermal Measurement, Modeling & Management Symposium (SEMI-THERM)*, San Jose, CA, USA, 2020, pp. 32-38, doi: 10.23919/SEMI-THERM50369.2020.9142831.

[5] Shahi, P., Agarwal, S., Saini, S., Niazmand, A., Bansode, P., & Agonafer, D., 2020, "CFD Analysis on Liquid Cooled Cold Plate Using Copper Nanoparticles," Proceedings of the ASME 2020 International Technical Conference and Exhibition on Packaging and Integration of Electronic and Photonic Microsystems. ASME 2020 International Technical Conference and Exhibition on Packaging and Integration of Electronic and Photonic Microsystems. Virtual, Online. October 27–29,2020.V001T08A007.
ASME. https://doi.org/10.1115/IPACK2020-2592

[6] Chu, R. C., Simons, R. E., Ellsworth, M. J., Schmidt, R. R., and Cozzolino, V., 2004, "Review of Cooling Technologies for Computer Products," IEEE Trans. Device Mater. Reliab., 4(4), pp. 568–585.

[7] Ellsworth, M. J., Campbell, L. A., Simons, R. E., Iyengar, M. K., Schmidt, R. R., and Chu, R. C., 2008, "The Evolution of Water Cooling for Large IBM Large Server Systems: Back to the Future," 11th Intersociety Conference on Thermal and Thermomechanical Phenomena in Electronic Systems (ITherm), Orlando, FL, May 28–31, pp. 266–274.

[8] McFarlane, R., 2012, "Will Water-Cooled Servers Make Another Splash in the Data Center?," Tech Target Network, Search Data Center, Newton, MA, accessed Feb. 26, 2012, https://searchdatacenter.techtarget.com/tip/Will-watercooled-servers-make-another-splash-in-the-data-center

[9] Schmidt, R. R., 2005, "Liquid Cooling Is Back," Electronics Cooling, 11(3), (epub).

[10] Patrizio, A., 2018, "Lenovo Introduces New Water-Cooled Server Technology," Network World, Framingham, MA, accessed Feb. 26, 2018, https://www.networkworld.com/article/3258646/data-center/lenovo-introduces-newwater-cooled-server-technology.html

[11] Koblentz, E., 2018, “How to Get Started With Liquid Cooling for Servers and Data Center Racks,” Data Centers Trends Newsletter, TechRepublic, US edition, accessed July 8, 2018, https://www.techrepublic.com/article/how-to-getstarted-with-liquid-cooling-for-servers-and-data-center-racks/

[12] Iyengar, M., David, M., Parida, P., Kamath, V., Kochuparambil, B., Graybill, D., Schultz, M., Gaynes, M., Simons, R., Schmidt, R., and Chainer, T., 2012, “Server Liquid Cooling With Chiller-Less Data Center Design to Enable Significant Energy Savings,” 28th Annual IEEE Semiconductor Thermal Measurement and Management Symposium (SEMI-THERM), San Jose, CA, Mar. 18–22, pp. 212–223.

[13] Fan, Y., Winkel, C., Kulkarni, D., and Tian, W., 2018, “Analytical Design Methodology for Liquid Based Cooling Solutions for High TDP CPUs,” 17th IEEE Intersociety Conference on Thermal and Thermomechanical Phenomena in Electronic Systems (ITherm), San Diego, CA, May 29–June 1, pp. 582–586.

[14] Shahi, P., Deshmukh, A. P., Hurnekar, H. Y., Saini, S., Bansode, P., Kasukurthy, R., and Agonafer, D. (November 22, 2021). "Design, Development, and Characterization of a Flow Control Device for Dynamic Cooling of Liquid-Cooled Servers." ASME. *J. Electron. Packag*. December 2022; 144(4): 041008. https://doi.org/10.1115/1.4052324

[15] Shahi, P., Saini, S., Bansode, P., and Agonafer, D., 2021, "A Comparative Study of Energy Savings in a Liquid-Cooled Server by Dynamic Control of Coolant Flow Rate at Server Level," in IEEE Transactions on Components, Packaging and Manufacturing Technology, 11(4), pp. 616-624, doi: 10.1109/TCPMT.2021.3067045

[16] Thirunavakkarasu, G., Saini, S., Shah, J.M., Agonafer, D., 2018, "Air Flow Pattern and Path Flow Simulation of Airborne Particulate Contaminants in a High-Density Data Center Utilizing Airside Economization," Proceedings of the ASME 2018 International Technical Conference and Exhibition on Packaging and Integration of Electronic and Photonic Microsystems. ASME 2018 International Technical Conference and Exhibition on Packaging and Integration of Electronic and Photonic Microsystems. San Francisco, California, USA. August 27–30, 2018. V001T02A011. ASME. https://doi.org/10.1115/IPACK2018-8436

[17]S. Saini, P. Shahi, P. Bansode, A. Siddarth, and D. Agonafer, “CFD Investigation of Dispersion of Airborne Particulate Contaminants in a Raised Floor Data The University of Texas at Arlington 701 S Nedderman Drive,” 2011.

[18] Saini, S., Shahi, P., Bansode, P., Siddarth, A., Agonafer, D., 2020, "CFD Investigation of Dispersion of Airborne Particulate Contaminants in a Raised Floor Data Center," 36th Semiconductor Thermal Measurement, Modeling & Management Symposium (SEMI-THERM), San Jose, CA, USA, 2020, pp. 39-47, doi: 10.23919/SEMITHERM50369.2020.9142865.

[19] Saini, S., Adsul, K.K., Shahi, P., Niazmand, A., Bansode, P., & Agonafer, D., 2020, "CFD Modeling of the Distribution of Airborne Particulate Contaminants Inside Data Center Hardware," Proceedings of the ASME 2020 International Technical Conference and Exhibition on Packaging and Integration of Electronic and Photonic Microsystems. ASME 2020 International Technical Conference and Exhibition on Packaging and Integration of Electronic and Photonic Microsystems. Virtual, Online. October 27–29, 2020. V001T08A005. ASME. https://doi.org/10.1115/IPACK2020-2590

[20] Saini, Satyam, 2018, “Airflow Path and Flow Pattern Analysis of Sub-Micron Particulate Contaminants in a Data Center with Hot Aisle Containment System Utilizing Direct Air Cooling,” The University of Texas at Arlington, Arlington, TX.

[21] Shah, J.M., Anand, R., Saini, S., Cyriac, R., Agonafer, D., Singh, P., & Kaler, M., 2019, "Development of a Technique to Measure Deliquescent Relative Humidity of Particulate Contaminants and Determination of the Operating Relative Humidity of a Data Center, " Proceedings of the ASME 2019 International Technical Conference and Exhibition on Packaging and Integration of Electronic and Photonic Microsystems. ASME 2019 International Technical Conference and Exhibition on Packaging and Integration of Electronic and Photonic Microsystems. Anaheim, California, USA. October 7–9, 2019. V001T02A016. ASME. https://doi.org/10.1115/IPACK2019-6601

[22] Saini, S., Shah, J. M., Shahi, P., Bansode, P., Agonafer, D., Singh, P., Schmidt, R., and Kaler, M. (September 15, 2021). "Effects of Gaseous and Particulate Contaminants on Information Technology Equipment Reliability—A Review." ASME. *J. Electron. Packag*. September 2022; 144(3): 030801. https://doi.org/10.1115/1.4051255

[23] Shah, JM, Bhatt, C, Rachamreddy, P, Dandamudi, R, Saini, S, & Agonafer, D. "Computational Form Factor Study of a 3rd Generation Open Compute Server for Single-Phase Immersion Cooling." Proceedings of the ASME 2019 International Technical Conference and Exhibition on Packaging and Integration of Electronic and Photonic Microsystems. ASME 2019 International Technical Conference and Exhibition on Packaging and Integration of Electronic and Photonic Microsystems. Anaheim, California, USA. October 7–9, 2019. V001T02A017. ASME. https://doi.org/10.1115/IPACK2019-6602

[24] Ansys® ICEPAK, Release 2019R3, ANSYS Icepak User’s Guide, [book and chapter reference name/numbers], ANSYS, Inc.

[25] Engineered Fluids Company EC – 100 Single Phase Immersion Cooling Fluids Data Sheet https://www.engineeredfluids.com/

[26] McWilliams, Trevor Dean. "Evaluating Heat Sink Performance In An Immersion-cooled Server System." (2014).

[27] Shinde, P.A., Bansode, P.V., Saini, S., Kasukurthy, R., Chauhan, T., Shah, J.M., & Agonafer, D., 2019, "Experimental Analysis for Optimization of Thermal Performance of a Server in Single Phase Immersion Cooling," Proceedings of the ASME 2019 International Technical Conference and Exhibition on Packaging and Integration of Electronic and Photonic Microsystems. ASME 2019 International Technical Conference and Exhibition on Packaging and Integration of Electronic and Photonic Microsystems. Anaheim, California, USA. October 7–9, 2019. V001T02A014. ASME. https://doi.org/10.1115/IPACK2019-6590

[28] Niazmand, A., Murthy, P., Saini, S., Shahi, P., Bansode, P., & Agonafer, D., 2020, "Numerical Analysis of Oil Immersion Cooling of a Server Using Mineral Oil and Al2O3 Nanofluid," Proceedings of the ASME 2020 International Technical Conference and Exhibition on Packaging and Integration of Electronic and Photonic Microsystems. ASME 2020 International Technical Conference and Exhibition on Packaging and Integration of Electronic and Photonic Microsystems. Virtual, Online. October 27–29, 2020. V001T08A009. ASME. https://doi.org/10.1115/IPACK2020-2662

[29] Bansode, Pratik V., Shah, Jimil M., Gupta, Gautam, Agonafer, Dereje, Patel, Harsh, Roe, David, and Tufty, Rick. "Measurement of the Thermal Performance of a Single-Phase Immersion Cooled Server at Elevated Temperatures for Prolonged Time." Proceedings of the ASME 2018 International Technical Conference and Exhibition on Packaging and Integration of Electronic and Photonic Microsystems. San Francisco, California, USA. August 27–30, 2018. V001T02A010. ASME.

[30] Most, Thomas, and Johannes Will. "Sensitivity analysis using the Metamodel of Optimal Prognosis." *Weimar Optimization and Stochastic Days* 8 (2011): 24-40.

[31] Niazmand, A., Chauhan, T., Saini, S., Shahi, P., Bansode, P.V., & Agonafer, D., 2020, "CFD Simulation of Two-Phase Immersion Cooling Using FC-72 Dielectric Fluid." Proceedings of the ASME 2020 International Technical Conference and Exhibition on Packaging and Integration of Electronic and Photonic Microsystems. ASME 2020 International Technical Conference and Exhibition on Packaging and Integration of Electronic and Photonic Microsystems. Virtual, Online. October 27–29, 2020. V001T07A009. ASME. https://doi.org/10.1115/IPACK2020-2595

[32] A. Lakshminarayana, A. Misrak, R. Bhandari, T. Chauhan, A. S. M. Raufur Chowdhury, and D. Agonafer, "Impact of Viscoelastic Properties of Low Loss Printed Circuit Boards (PCBs) on Reliability of WCSP Packages Under Drop Test," in 2020 IEEE 70th Electronic Components and Technology Conference (ECTC), Jun. 2020, vol. 2020-June, pp. 2266–2271, doi: 10.1109/ECTC32862.2020.00353.

[33] T. Chauhan, R. Bhandari, K. B. Sivaraju, A. S. M. R. Chowdhury, and D. Agonafer, "IMPACT OF IMMERSION COOLING ON THERMOMECHANICAL PROPERTIES OF LOW-LOSS MATERIAL PRINTED CIRCUIT BOARDS," J. Enhanc. Heat Transf., vol. 28, no. 7, pp. 73–90, 2021, doi: 10.1615/JEnhHeatTransf.2021039486.

[34] S. Ramdas, A. S. M. R. R. Chowdhury, A. Lakshminarayana, R. Bhandari, A. Misrak, and D. Agonafer, "IMPACT OF THERMAL AGING ON THERMOMECHANICAL PROPERTIES OF OIL-IMMERSED PRINTED CIRCUIT BOARDS," in SMTA International, 2019, pp. 772–778.

[35] S. Dhandarphale, T. Chauhan, A. S. M. R. Chowdhury, and D. Agonafer, "IMPACT OF SINGLE-PHASE IMMERSION COOLING ON COEFFICIENT OF THERMAL EXPANSION OF PCBS AND IMPACT OF CHANGE IN THEMO-MECHANICAL PROPERTIES ON RELIABILITY OF SECOND LEVEL SOLDER JOINT OF BGA PACKAGE University of Texas at Arlington," in SMTA International, 2020, pp. 408–412.